Chapter 17

Active R and Active C Filters

17.1 Introduction

Conventionally, the design of OA-RC (operational amplifiers with resistors and capacitors) circuits assumes that OAs are ideal, having a large frequency independent gain. However, a commercially integrated OA is a non-ideal device, whose gain is frequency dependent and exhibits a LP (low pass) characteristic. A simple model for OAs, given in Chapter 1, is repeated here depicting its frequency dependent gain nature.

$$A(s) = \frac{A_o \omega_a}{s + \omega_a} \cong \frac{B}{s} \tag{17.1}$$

In equation (17.1), ω_a is its first pole, A_o is the gain at dc and $B = A_o\omega_a$ is gain bandwidth product. This effect of the gain bandwidth product, *B,* being finite, its effect on the magnitude and phase responses of the filter became important criterion for comparison of the performance of filters. Finite *B* restricts the frequency range of the operation of OA-RC filters to mostly the audio frequency range, particularly when commercially economical OAs, such as OA 741, are used. In fact, in some topologies, product of pole-*Q* and center frequency ω_o has to be much less than *B* to avoid undesirable enhancement in *Q*, and likely instability. Consequently, suitable compensating schemes were developed to design filters with lesser dependence on OA gain characteristics, like those shown for integrators in Chapter 2; in other cases, specially designed but costly OAs were used.

In an alternative approach, instead of considering the frequency dependent gain of the OA as undesirable, it has been exploited by using it directly in the design itself. This approach increases the frequency range of operation, and also reduces or completely eliminates the

https://doi.org/10.1017/9781108762632.018 Published online by Cambridge University Press

requirement of external capacitors. In this context, networks which use only OAs and resistors, with no external capacitors in their implementation, and derive their response from the internal dynamics of the OAs, are known as *active R circuits* [17.1], [17.2].

Similar to active R, *active C networks* have also been designed. They utilize the frequency dependent model of the OAs, but use only capacitances, mostly in ratio form. It results in an extended frequency range; the use of small value capacitors in ratio form provides related advantages.

17.2 Basic Techniques in Active R Synthesis

Active R synthesis is an off-shoot of the active RC synthesis, where external capacitors were eliminated. Hence, the techniques used in the active RC synthesis are only tailored to suit active R realizations; these are briefly discussed in this section.

The active R realization approaches can be broadly classified as (i) the *direct form* and (ii) the *cascade form*. As in the OA-RC case, a resistively terminated LC ladder is very commonly used as the basic starting structure in the active R and active C direct form approach. The direct form approach can be further classified into (a) the simulated immittance (inductance and capacitance using OAs and resistors) and (b) the frequency dependent negative resistance (FDNR) approach. For the immittance simulation approach, GI (grounded inductance) and FI (floating inductance) simulation is discussed in Section 17.4 using OAs and resistances (ratios). OA R simulation of FDNR in grounded and floating form is show in Section 17.5. In active R synthesis, as capacitors are also not used, simulation of capacitors in grounded and floating form is discussed in Section 17.6. All the simulated elements are then employed to describe the immittance simulation and the FDNR approaches in Section 17.7. In the cascade synthesis process, active R building blocks (first-order and second-order filter sections) are connected in a non-interactive cascade form to realize higher-order filters; they are discussed in Sections 17.8–10.

Certain limitations of the OA R/OA C circuits are described at the end of the chapter along with some of the methods to overcome these limitations.

17.3 Direct Form of Active R Synthesis

In network realizations using the direct form of active R synthesis approach, the problem effectively reduces to the simulation of inductors and capacitors (and FDNRs) using OAs and resistors. While designing these elements, it is desirable that the simulators possess the same qualities as required in the OA-RC case, such as: (i) low sensitivities, (ii) stability, (iii) reliable high frequency performance, (iv) use of a smaller number of active and passive components, (v) suitability to IC (integrated circuits) implementation, (vi) high dynamic range and (vii) non-critical component or gain matching. It is rare for a circuit to possess all the aforementioned attractive properties simultaneously. In this chapter, only a few active R grounded and floating

https://doi.org/10.1017/9781108762632.018 Published online by Cambridge University Press

component simulators will be discussed; a large number of component simulators are available in literature.

17.4 Inductance Simulation

Grounded Inductance, GI-1: A GI simulator is shown in Figure 17.1(a)[17.3]. Using the approximated first-pole roll-off model of the OA of equation (17.1), input impedance is found as:

$$Z_{\text{in}}(s) = k\frac{s\tau_1 + 1}{s\tau_2 + 1} \tag{17.2}$$

$$k = (a_2/(b_2)),\ \tau_1 = (a_1/BR_1\ R_3), \text{ and } \tau_2 = (R_1/(BR_3)) \tag{17.3a}$$

$$a_1 = R_1(R_2 + R_3 + R_4) + R_2\ (R_3 + R_4),\ a_2 = a_1 + A_o\ R_1\ R_3 \tag{17.3b}$$

$$b_1 = (R_2 + R_3 + R_4),\ b_2 = b_1 + A_o\ R_3 \tag{17.3c}$$

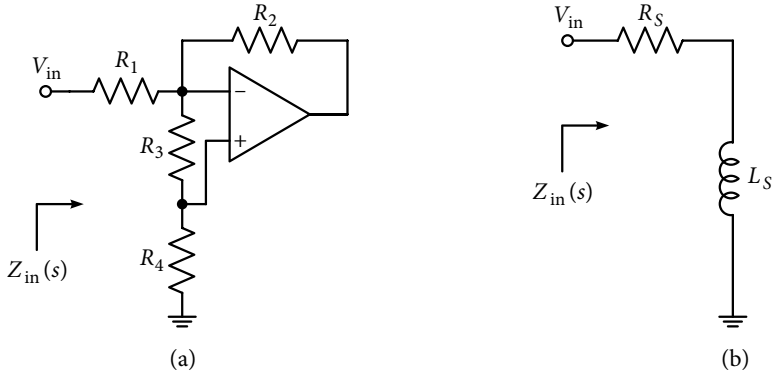

Figure 17.1 (a) Grounded inductance simulator G I-1 and (b) equivalent circuit of the non-ideal inductor.

Input impedance in equation (17.2) satisfies the condition of a bilinear RL function when $k > 0$ and $\tau_1 > \tau_2 \geq 0$. For $s = j\omega$, we can express $Z_{\text{in}}(j\omega)$ as:

$$Z_{\text{in}}(j\omega) = R_s + j\omega L_s,\ Q = (\omega L_s/R_s) \tag{17.4}$$

Series form of the equivalent circuit of the simulated GI is shown in Figure 17.1(b), and the parameters L_s and Q are obtained from equations (17.2) and (17.3), which are frequency dependent.

https://doi.org/10.1017/9781108762632.018 Published online by Cambridge University Press

$$L_s = \frac{R_2\left(1+R_4/R_3\right)}{B\left\{1+\left(1+\frac{R_2}{R_3}+\frac{R_4}{R_3}\right)^2\left(\frac{\omega}{B}\right)^2\right\}} \cong \frac{R_2\left(1+R_4/R_3\right)}{B} \tag{17.5}$$

$$Q = \left(\frac{\omega}{B}\right)\frac{\left(R_2/R_1\right)\left(1+R_4/R_3\right)}{1+\left(R_2/R_1\right)\left(1+R_4/R_3\right)\left(1+\frac{R_2}{R_3}+\frac{R_4}{R_3}\right)\left(\frac{\omega}{B}\right)^2} \tag{17.6}$$

It is observed from equation (17.5) that the inductor is realizable even when $R_1 = 0$; however, with the incorporation of R_1, independent tuning of the quality factor Q is possible. While designing the GI simulator, the ratios (R_2/R_3) and (R_4/R_3) are to be pre-selected. The value of L_s is tuned with R_2 and can be further increased by having larger values for the ratio (R_4/R_3). However, the ratio (R_4/R_3) affects Q at high working frequency. Generally, a convenient pre-selection in the design is $(R_4/R_3) = (R_2/R_3) = 1$.

Simulation of Floating Inductance FI-1: FI-1 is realized using GI-1 by un-grounding resistor R_4 in Figure 17.1(a), and connecting it back-to-back with another GI-1, forming a two-port network as shown in Figure 17.2(a). Analysis of the circuit, using an approximate model of the OA, $A(s) \cong \frac{B}{s}$, gives the short circuit admittance parameters matrix as:

$$\left[y_{FI-1}\right] = \frac{1}{2k}\frac{s\tau_1+1}{s\tau_2+1}\begin{bmatrix} 1 & -1 \\ -1 & 1 \end{bmatrix} \tag{17.7}$$

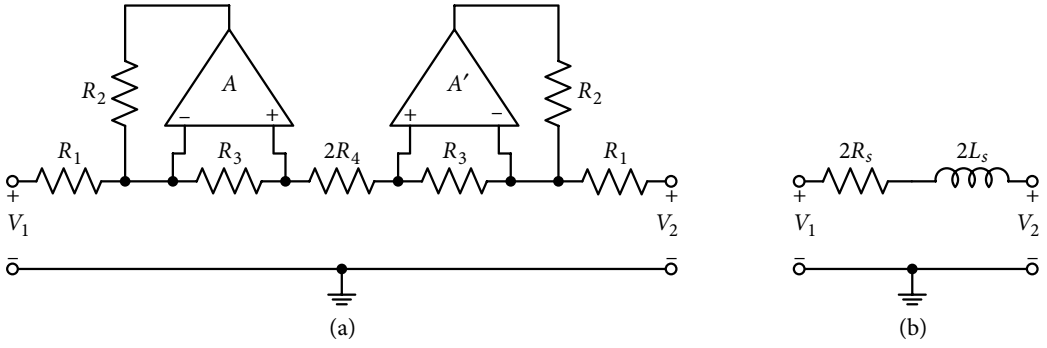

Figure 17.2 (a) Simulation of floating inductance FI-1 by ungrounding resistor R_4 of Figure 17.1(a) and connecting it back-to-back; (b) series form equivalent circuit of the non-ideal floating inductor.

where k, τ_1 and τ_2 are given by equation (17.2) and (17.3); equation (17.7) is obtained after simplification of the y parameters. Under the satisfying condition of equation (17.8), parameters of the equivalent floating inductor FI-1 are as given in equation (17.9), and shown in Figure 17.2(b).

https://doi.org/10.1017/9781108762632.018 Published online by Cambridge University Press

$$\left(R_2 / R_1\right) \gg 1 \text{and } \omega^2 \ll \left(BR_3 / R_4\right)^2 \tag{17.8}$$

$$L_{FI} = 2L_s \text{ and } Q_{FI} = Q \tag{17.9}$$

Here L_s and Q are given by equations (17.5) and (17.6). The useful frequency range of the FI-1 is given by equation (17.8). For the 741 type of OAs, the circuit gives reliable performance over a range of about 200 kHz; considerably more than the conventional OA-RC case.

It was assumed that back-to-back connected blocks were identical, that is, components were matched. However, in practice, the two blocks may have some mismatch. Simple analysis shows that the circuit still simulates floating inductance provided:

$$y_{11}' y_{22} = y_{11} y_{22}' \tag{17.10}$$

where primed parameters belong to the non-identical block.

Example 17.1: Figure 17.3(a) shows a passive HPF (high pass filter) circuit. Obtain the characteristic of its active version using GI-1. Value of the cut-off frequency needs to be 200 krad/s.

Solution: Transfer function of the passive circuit is derived as:

$$\frac{V_{\text{out}}}{V_{\text{in}}} = \frac{\left(1/CR\right)s^2 + \left(R_s / L\right)s}{s^2 + \left(R_s / L\right)s + 1/LC} \tag{17.11}$$

From equation (17.11), expression of the parameters of the HPF are:

$$\omega_o^2 = \frac{1}{LC}, \; Q = \frac{1}{R_s}\sqrt{\left(L/C\right)} \tag{17.12}$$

For a selected value of C = 10 nF, equation (17.12) gives L = 2.5 mH.

From equation 17.5(b), with $B = 2\pi \times 10^6$ rad/s, and a pre-selected value of R_2 = 10 kΩ.

$$\frac{R_4}{R_3} = \frac{BL_s}{R_s} - 1 = \frac{4}{7}$$

Hence, if R_4 is selected as 4 kΩ, R_3 = 7 kΩ. Resistance R_1 is selected as 0.1 kΩ to keep the series resistance with the inductor small.

https://doi.org/10.1017/9781108762632.018 Published online by Cambridge University Press

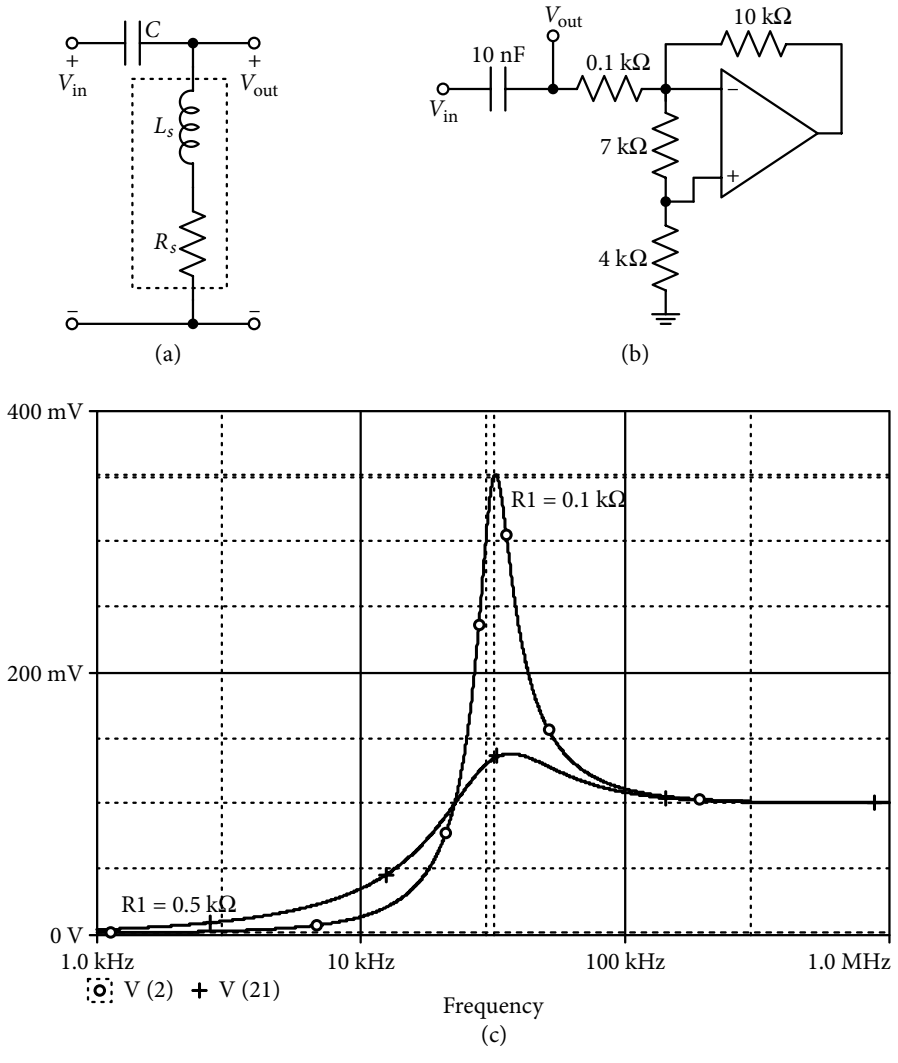

Figure 17.3 (a) A passive high pass filter and (b) its active R version using grounded inductor FI-1. (c) PSpice simulation of the high pass filter (Example 17.1) using GI-1 with resistance R_1 = 0.1 kΩ and 0.5 kΩ.

Simulated response of the HPF is shown in Figure 17.3(c), in which peak occurs at f_{peak} = 32.219 kHz. Gain at the peak is 3.511, so the realized value of $Q \cong 3.511$, and application of equation (3.46) gives the resonance frequency as:

$$f_o = f_{\text{peak}} \Big/ \sqrt{\left(1 - \frac{1}{2Q^2}\right)} = 32.219\left\{1 - \frac{1}{2(3.511)^2}\right\}^{-½} = 31.56 \text{ kHz}$$

https://doi.org/10.1017/9781108762632.018 Published online by Cambridge University Press

Simulated peak frequency is 198.77 krad/s against the design value of 200 krad/s.

Effective series resistance of the simulated inductor R_s is found using equation (17.12) as:

$$R_s = \frac{1}{3.382}\left(\frac{2.5\times10^{-3}}{10^{-8}}\right)^{½} = 147.8\Omega$$

To exhibit the control of the quality of the simulated inductance by R_1, it is now selected as 0.5 kΩ. With all other components remaining the same, response of the modified HPF is also shown in Figure 17.3(c). Now f_{peak} is 36.94 kHz, and peak gain is 1.3808 (or $Q \cong 1.3808$).

From equation (17.10), effective series resistance R_s in this case is:

$$R_s = \frac{1}{1.3808}\left(\frac{2.5\times10^{-3}}{10^{-8}}\right)^{½} = 362.1\Omega$$

Low Component Floating Inductance FI-2: The floating inductor FI-1 has a number of attractive features, such as stability, low sensitivity, and reliable high frequency performance. Moreover, critical component matching is not required. However, the circuit uses seven resistances with sufficiently high resistance spread. Floating inductance FI-2, which we will discuss now, retains most of the desirable qualities of the FI-1. In addition, it uses a minimum number of components; only two OAs and two equal value resistances[17.2] [17.4].

An inductance simulator FI-2 is shown in Figure 17.4(a). For working frequency $\omega \gg \omega_a$, and $A \cong B/s$ for the OAs, analysis gives its short-circuit admittance matrix as:

$$[y] = \begin{bmatrix} \frac{s+B}{sR} & -\frac{B}{sR} \\ -\frac{B'}{sR'} & \frac{s+B'}{sR'} \end{bmatrix} \tag{17.14}$$

For nominal element values, $R = R'$ and $B = B'$, equation (17.14) simplifies to:

$$[y] = \frac{1}{sR}\begin{bmatrix} (s+B) & -B \\ -B & (s+B) \end{bmatrix} \tag{17.15}$$

In the sinusoidal case, with $\omega \ll B$ (say $\leq 0.1B$), deviations in the magnitude of elements in equation (17.15) are less than 1%, and the equation (17.15) modifies to:

$$[y(j\omega)] = \left(\frac{1}{R} + \frac{B}{j\omega R}\right)\begin{bmatrix} 1 & -1 \\ -1 & 1 \end{bmatrix} \tag{17.16}$$

https://doi.org/10.1017/9781108762632.018 Published online by Cambridge University Press

Equation (17.16) represents a lossy FI, and its equivalent in series form is shown in Figure 17.4(c); the parameters are:

$$L_s = \frac{BR}{\left(\omega^2 + B^2\right)}, \quad R_s = \frac{\omega^2 R}{\left(\omega^2 + B^2\right)}, \quad Q = \frac{B}{\omega} \tag{17.17}$$

The circuit is suitable for realizing very high Q values at comparatively lower frequencies. For example, for an OA with $B = 2\pi \times 10^6$ rad/s, $Q > 100$ is realizable at frequencies below 10 kHz. Thus, in the working frequency range of available active RC FIs ($f < 5$ kHz with the same type of OAs), FI-2 realizes very high Q and behaves as a nearly lossless inductor (except at very low frequencies close to ω_a, where the approximated model of OA does not remain valid).

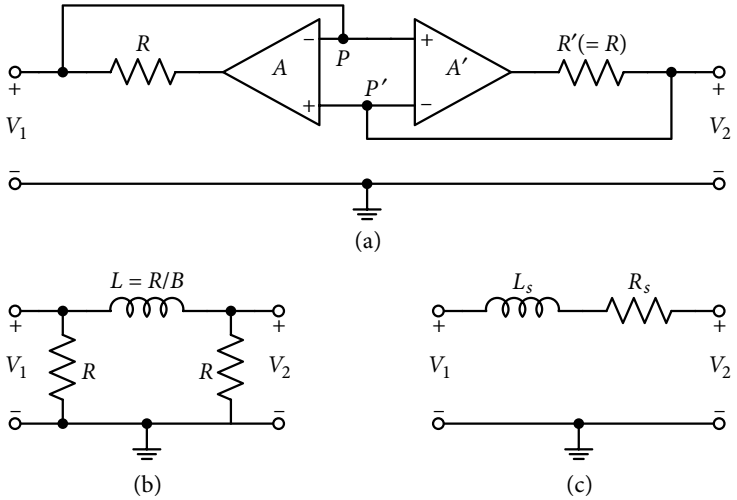

Figure 17.4 (a) Low component floating inductance simulator FI-2, (b) its passive equivalent without mismatch ($R' = R$), and (c) series equivalent of FI-2.

Low Component Grounded Inductance GI-2: FI-2 has the versatility of conversion to GI. Two identical GIs may be obtained from the FI-2 by pulling out the non-inverting terminal P and P' of the OAs in Figure 17.4(a) and connecting to the ground. The resulting GI-2 simulator is shown in Figure 17.5(a) [17.2]. Its analysis gives the RL-driving point admittance:

$$Y_{\text{in}}(s) = \frac{1}{R} + \frac{B}{sR} \tag{17.18}$$

Its passive equivalent is shown in Figure 17.5(b).

https://doi.org/10.1017/9781108762632.018 Published online by Cambridge University Press

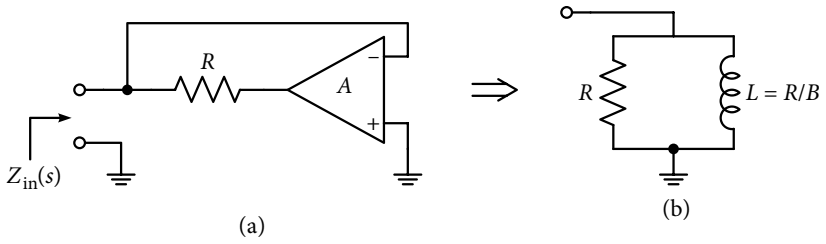

Figure 17.5 (a) GI-2 obtained from FI-2 of Figure 17.4(a) and (b) its parallel form passive equivalent.

Example 17.2: Obtain a fifth-order LP Chebyshev filter using FI-2, having a pass band edge frequency of 100 krad/s and ripple width of 0.5 dB.

Solution: Minimum inductance fifth-order ladder for realizing Chebyshev response with 0.5 dB ripple is taken from Table 3.5(b) and shown in Figure 17.6(a). Element values for the normalized ladder are:

$$R_{in} = R_L = 1\ \Omega,\ C_1 = C_5 = 1.7058\ \text{F},\ C_3 = 2.5408\ \text{F},\ L_2 = L_4 = 1.2296\ \text{H} \tag{17.19}$$

Elements are frequency scaled by a factor of 100 krad/s, and further, impedance scaled by 1 kΩ, which results in the following de-normalized element values:

$$R_{in} = R_L = 1\ \text{k}\Omega,\ C_1 = C_5 = 17.058\ \text{nF},\ C_3 = 25.408\ \text{nF},\ L_2 = L_4 = 12.29\ \text{mH} \tag{17.20}$$

With de-normalized element values, the fifth-order active R filter realized through using two active R FIs, is shown in Figure 17.6(b). Using equation (17.17), the FIs will employ resistances of 77.36 kΩ.

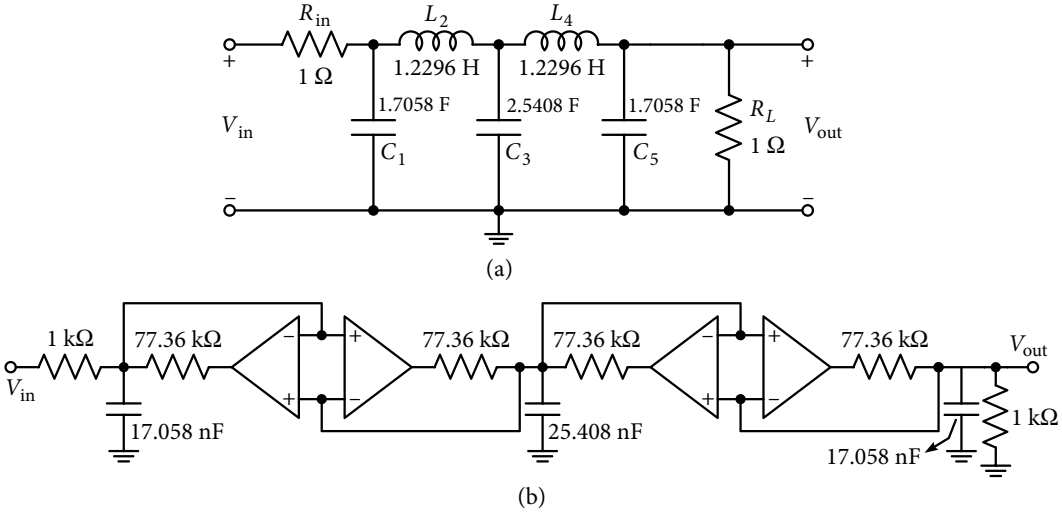

https://doi.org/10.1017/9781108762632.018 Published online by Cambridge University Press

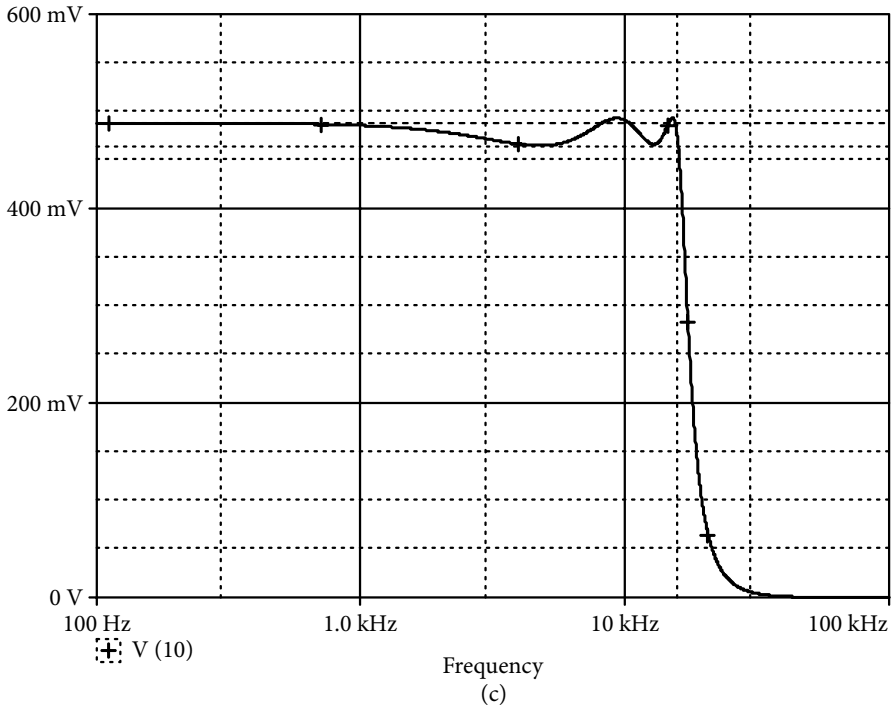

Figure 17.6 (a) Fifth-order Chebyshev filter ladder structure, and (b) its active R realization employing FI-2. (c) Fifth-order Chebyshev filter response employing FI-2 in Example 17.2.

The PSpice simulated response is shown in Figure 17.6(c). The simulated pass band edge frequency is 15.532 (97.63 krad/s) and ripple width is 0.471 dB. Important parameters are very close to the design; however, low frequency gain is 0.487, instead of 0.5, most likely due to parasitic resistance associated with the simulated FI-2, which was shown in Figures 17.4(b)–(c).

17.5 Active R Frequency Dependent Negative Resistance (FDNR)

The frequency dependent negative resistance (FDNR) approach to active RC synthesis, given by Bruton [9.8], is particularly useful when the filter contains a large number of FIs, which get converted to resistors. A number of reliable active RC circuits are available for grounded and floating FDNRs. However, conventional limitations of active RC circuits, mainly the low frequency range of operation, are present. Moreover, the large component count, particularly the use of two external capacitors for grounded FDNR, is not an attractive feature for integration. It has been observed that active R circuits for FDNR simulation can obviate the mentioned drawbacks to a large extent.

https://doi.org/10.1017/9781108762632.018 Published online by Cambridge University Press

Grounded FDNR Simulation: An active R circuit for the simulation of a grounded FDNR is shown in Figure 17.7(a) [17.5]. Straightforward analysis of the circuit, using the approximated model of the OA of equation (17.1), gives the driving point impedance as:

$$Z_{\text{in}} = R + (D/s^2) \tag{17.21}$$

$$\text{where, } R = R_D + R_o,\ D = B_1\ B_2\ R_D \tag{17.22}$$

Here, R_o is the output resistance of OA2 and B_1, B_2 are the respective gain bandwidth of OA1 and OA2. Equation (17.21) represents a non-ideal FDNR having a series positive resistance R. For sinusoidal excitation, the frequency dependent impedance of the circuit shall be:

$$Z_{\text{in}}(j\omega) = (R_D + R_o) - (B_1\ B_2\ R_D/\omega^2) \tag{17.23}$$

It may be noted that the circuit will exhibit zero impedance at a certain frequency ω_s as:

$$\omega_s = \left\{B_1 B_2 R_D / \left(R_D + R_o\right)\right\}^{1/2} \tag{17.24}$$

Similar to the quality factor of inductors, a figure of merit to evaluate the quality of the FDNR is given as:

$$F_D = -\frac{\text{Negatve resistance at frequency } \omega}{\text{Series resistance}} = -\frac{B_1 B_2}{\omega^2}\left(\frac{R_D}{R_D + R_o}\right) \tag{17.25}$$

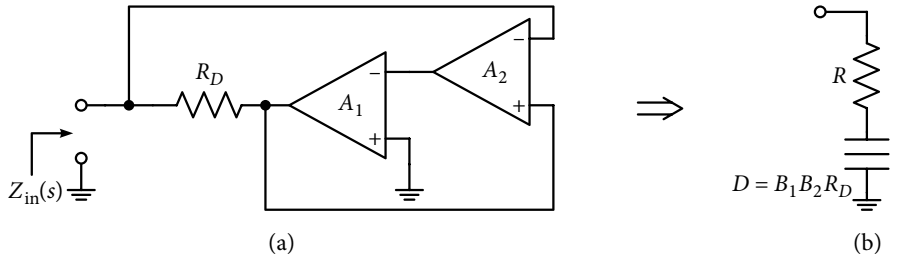

Figure 17.7 (a) Active R grounded FDNR simulator and (b) its equivalent representation.

Floating FDNR Simulation: As in the case of active RC, the grounded FDNR circuit of Figure 17.7(a) may be used to form a floating FDNR circuit as shown in Figure 17.8(a) [17.5]. Assuming similar blocks on both sides of the dotted line, analysis of the circuit using $A \cong B/s$, gives the parameters of the floating FDNR, same as that for the grounded FDNR.

$$R = R_D + R_o,\ D = B_1 B_2 R_D \tag{17.25}$$

https://doi.org/10.1017/9781108762632.018 Published online by Cambridge University Press

The circuit is absolutely stable, enjoys low active and passive sensitivities, and is useful for a large frequency range.

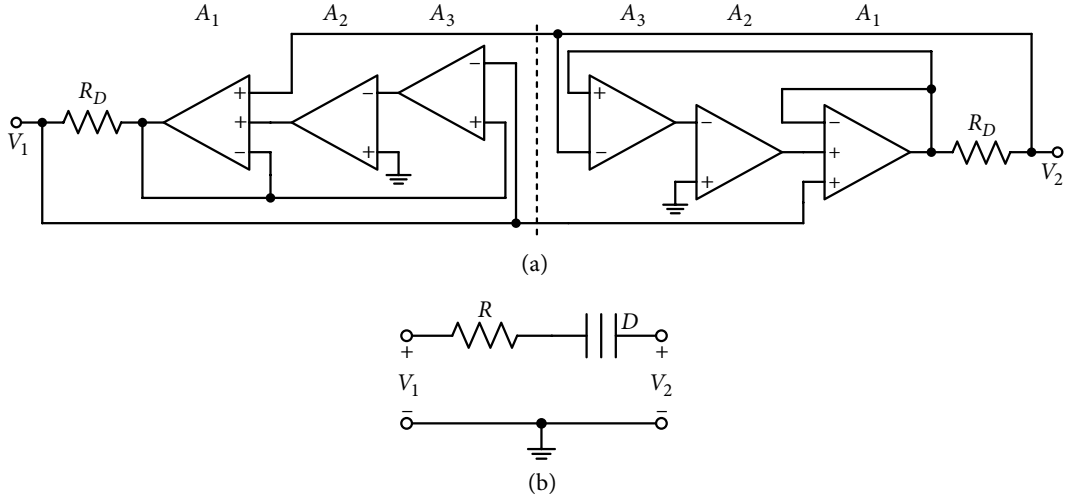

Figure 17.8 (a) Active R floating FDNR simulator and (b) its equivalent representation.

Example 17.3: Redesign the filter of Example 17.2 with a pass band edge frequency of 200 krad/s, using grounded FDNRs.

Solution: To realize the filter circuit using grounded FDNR, the passive structure in Figure 17.6(a) is scaled by s. The resulting circuit is shown in Figure 17.9(a), with the normalized circuit elements as:

$$C_{\text{in}} = C_L = 1 \text{ F}, R_2 = R_4 = 1.2296\ \Omega, D_1 = D_5 = 0.5862, D_3 = 0.39357 \tag{17.25}$$

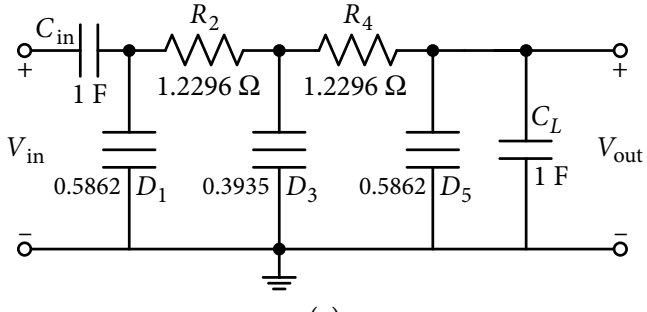

https://doi.org/10.1017/9781108762632.018 Published online by Cambridge University Press

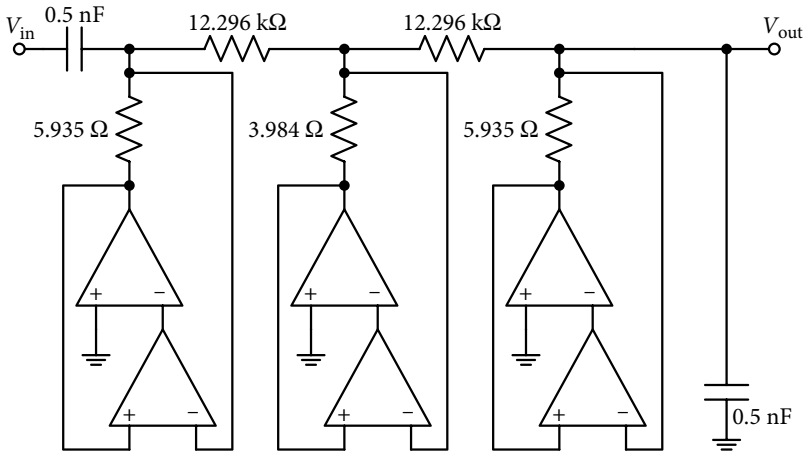

(b)

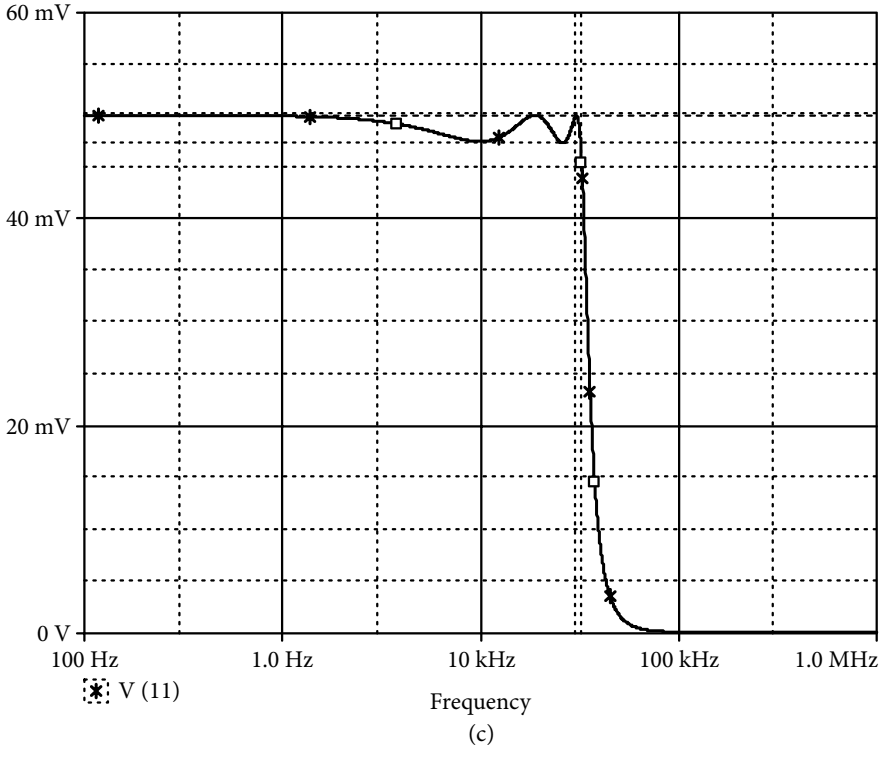

(c)

Figure 17.9 (a) Fifth-order Chebyshev filter ladder obtained after frequency transformation from Figure 17.6(a). (b) De-normalized version with FDNRs using active R circuit. (c) Simulated magnitude response of the fifth-order Chebyshev filter using grounded FDNRs: example 17.3.

https://doi.org/10.1017/9781108762632.018 Published online by Cambridge University Press

The active *R* version of the filter is shown in Figure 17.9(b), which employs grounded FDNR of Figure 17.7(a). Its resistances are calculated using equation (17.22):

$$R_{D1,5} = \frac{0.5862}{\left(2\pi \times 10^6\right)^2} \text{ and } R_{D3} = \frac{0.39357}{\left(2\pi \times 10^6\right)^2}$$

Applying impedance scaling of 10^4 and frequency scaling of 2×10^5, element values are

$$C_{\text{in}} = C_L = 0.5 \text{ nF}, R_2 = R_4 = 12.296 \text{ k}\Omega, R_{D1,\,5} = 5.935\ \Omega, R_{D3} = 3.984\ \Omega.$$

Simulated magnitude response of the active R filter is shown in Figure 17.9(c). Simulated pass band edge frequency is 31.996 (201.1 krad/s) and the ripple width is 2.523 mV for maximum output of 49.9 mV, which corresponds to 0.45 dB.

17.6 Active R Capacitors

Micro miniaturized capacitors occupy large chip area as compared to active devices. For economic reasons, it is therefore, not only desirable to reduce the number of capacitors, but also the total capacitance on the chip. The concept of eliminating external capacitors, without compromising any of the desirable qualities with them is very attractive. Hence, stable C simulators for grounded and floating capacitors (FCs) will be discussed in this chapter.

Simulation of Grounded Capacitor GC-1: A simple circuit, shown in Figure 17.10(a) is given for the simulation of grounded capacitor (GC) using only one OA and one resistor. With the OA characterized by its first-pole roll-off model, input impedance is obtained as:

$$Z_{\text{in}}(s) = R_c\left(1 + \frac{B}{s + \omega_a}\right) \tag{17.26}$$

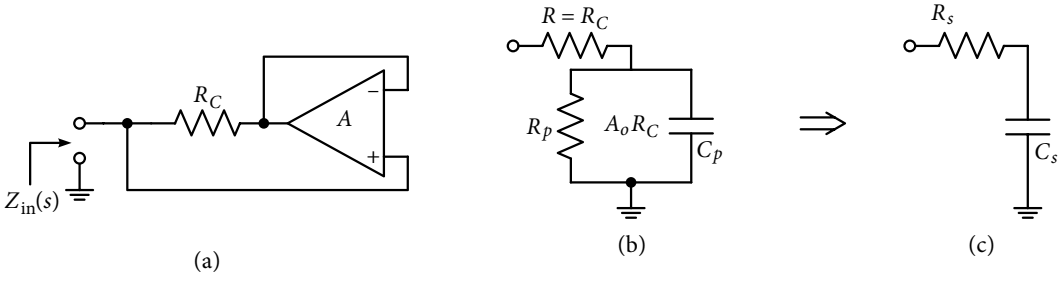

Figure 17.10 (a) Grounded capacitance simulator GC-1, using a single OA; (b) its parallel form equivalent circuit and (c) series form equivalent circuit.

https://doi.org/10.1017/9781108762632.018 Published online by Cambridge University Press

Equation (17.26) represents a lossy capacitor, and its equivalent is shown in Figure 17.10(b). The parameters are:

$$C_p = \frac{1}{BR_c},\ R_p = A_o R_c \text{ and } R = R_c \tag{17.27}$$

Its series form equivalent impedance as shown in Figure 17.10(c) is given as:

$$Z_{\text{in}}(j\omega) = R_s + (1/j\omega C_s) \tag{17.28}$$

$$\text{where, } C_s = \frac{\omega^2 + \omega_a^2}{B\omega^2 R_c} \cong \frac{1}{BR_c} \tag{17.29}$$

$$R_s = R_c \frac{\omega^2 + \omega_a^2 + B\omega_a}{\omega^2 + \omega_a^2} \cong R_c\left(1 + \frac{B\omega_a}{\omega^2}\right) \tag{17.30}$$

This gives the quality factor of the simulated capacitor as:

$$Q = \frac{1}{\omega C_s R_s} = \frac{B\omega}{\omega^2 + \omega_a^2 + B\omega_a} \cong \frac{B\omega}{\omega^2 + B\omega_a} \tag{17.31}$$

For $B = 2\pi \times 10^6$ rad/s and $\omega_a = 2\pi \times 10$ rad/s, equation (17.31) shows that the quality factor has a maximum value of nearly 158 at 3.16 kHz and decreases on both sides of the peak value frequency.

It is easily observable that the GC simulator GC-1 uses a minimum number of active and passive components. However, for some applications, where capacitor quality requirements are stringent, it may not be recommended. Hence, a high-quality GC simulator using two OAs will be studied next.

Simulation of High-Quality Grounded Capacitor GC-2: The GC-2 simulator for the simulation of high-Q values is shown in Figure 17.11 [17.6]. It can be analyzed for different values of gain bandwidth products for the two OAs used. However, without any loss of generality, assuming identical OAs ($B_2 = B_1$) and ($\omega_{a1} = \omega_{a2}$), analysis gives input impedance as:

$$Z_{\text{in}}(s) = R_c\left\{1 + \frac{B^2}{(s + \omega_a)(s + \omega_a + B)}\right\} \tag{17.32}$$

For sinusoidal excitation, equation (17.32) simplifies as:

$$Z_{\text{in}}(j\omega) = R_s + 1/j\omega C_s \tag{17.33}$$

https://doi.org/10.1017/9781108762632.018 Published online by Cambridge University Press

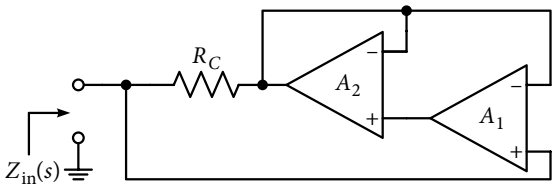

Figure 17.11 High-quality grounded capacitance simulator, GC-2.

Expressions for the equivalent series resistance R_s and simulated capacitance C_s are:

$$R_s = R_c \frac{\omega^4 + B^3\omega_a}{\omega^2(\omega^2 + B^2)} \tag{17.34}$$

$$C_s = \frac{(\omega^2 + B^2)}{B^3 R_c} \tag{17.35}$$

Hence, quality of the capacitor is obtained as:

$$Q = \frac{\omega B^3}{\omega^4 + B^3\omega_a} \tag{17.36}$$

From equation (17.36), finite maximum Q, and the frequency at which it occurs, are:

$$Q_m = 0.25\left(3B / \omega_a\right)^{\frac{3}{4}} \tag{17.37}$$

$$\omega_m = \left(B^3\omega_a / 3\right)^{\frac{1}{4}} \tag{17.38}$$

For nominal parameters of the 741/747 type of OAs, Q_m and ω_m are, respectively 3200 and 43 kHz, which reflects a sufficiently good quality; even better than many practical realizations of capacitors over a large frequency range.

Simulation of Floating Capacitor FC: Similar to the cases of FI or floating FDNR, the circuit for floating capacitor (FC) employs a larger number of elements and requires some form of matching of elements. Figure 17.12 shows a circuit for the simulation of FC [17.2]. Employing the first-pole roll-off model for the OAs, and assuming matched elements and OAs on the two halves of the circuit (primed and un-primed being the same), short circuit admittance parameters are found as:

$$y_{11} = y_{22} = \frac{\left\{\left(1+r_1\right)\left(s+\omega_{a2}\right)+r_1B_2\right\}\left(s+\omega_{a1}\right)}{R_c\left\{\left(1+r_1\right)\left(s+\omega_{a1}\right)\left(s+\omega_{a2}\right)+r_1B_2\left(s+\omega_{a1}\right)+B_1B_2\right\}} \tag{17.39}$$

https://doi.org/10.1017/9781108762632.018 Published online by Cambridge University Press

$$-y_{12} = -y_{21} = \frac{\left\{\left(1+r_1\right)/\left(1+r_2\right)\right\} r_2 B_2 \left(s+\omega_{a1}\right)}{R_c\{\left(1+r_1\right)\left(s+\omega_{a1}\right)\left(s+\omega_{a2}\right)+r_1 B_2\left(s+\omega_{a1}\right)+B_1 B_2\}} \tag{17.40}$$

where, $r_1 = R_2/R_1$ and $r_2 = R_4/R_3$.

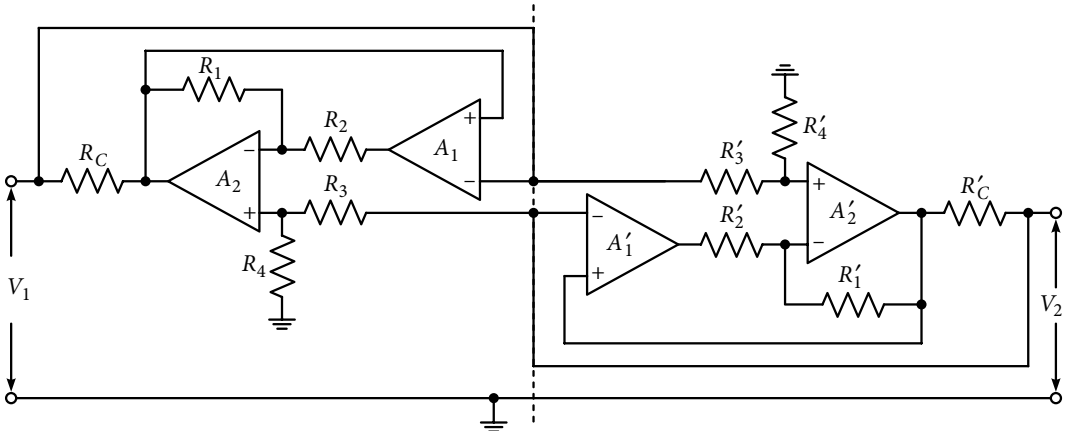

Figure 17.12 Active R floating capacitance simulator for high-frequency operation.

To ensure that the circuit simulates the capacitor, the *y* parameters must satisfy the following conditions:

i. $y_{11} = -y_{12} = -y_{21} = y_{22}$ (17.41a)

ii. y_{11} yields an RC admittance function (17.41b)

Conditions in equation (17.41) are satisfied (while primed and un-primed elements are the same) when the following relation is satisfied:

$$(1 + r_1)(s + \omega_{a2}) + r_1 B_2 = \{(1 + r_1)/(1 + r_1)\} r_2 B_2 \tag{17.42}$$

If, $r_1 = r_2 = r$, equation (17.42) simplifies as:

$$(1 + r)(s + \omega_{a2}) + rB_2 = rB_2 \tag{17.43}$$

The condition in equation (17.43) is satisfied in the following frequency range, which represents the useful frequency range of the operation of the FC.

$$\omega_a^2 \ll \omega^2 \ll \left\{rB_2/\left(1+r\right)\right\}^2 \tag{17.44}$$

https://doi.org/10.1017/9781108762632.018 Published online by Cambridge University Press

For sinusoidal operation:

$$Z_{11}(s) = \left.\frac{1}{y_{11}(s)}\right|_{s=j\omega} = R_s + \frac{1}{j\omega C_s} \tag{17.45}$$

where R_s and C_s are the effective series resistance and capacitance, which are derived from equation (17.39) while applying the condition of equation (17.43) as:

$$R_s = R_c \frac{(1+r)^2\omega^4 + B^3\omega_a r + \left(r^2 - r - 1\right)(\omega B)^2}{(1+r)^2\omega^4 + \left(\omega^2 + \omega_a^2\right)(Br)^2} \tag{17.46}$$

$$C_s = \frac{1}{R_c}\frac{(1+r)^2\omega^4 + \left(\omega^2 + \omega_a^2\right)(Br)^2}{rB^3\omega^2} \tag{17.47}$$

Quality factor of the FC is obtained as:

$$Q = \frac{\omega B^3}{(1+r)^2\omega^4 + B^3\omega_a r + \left(r^2 - r - 1\right)(\omega B)^2} \tag{17.48}$$

Equation (17.47) can be approximated for the frequency range, $\omega^2 \gg \omega_a^2$ as:

$$C_s \cong r/BR_c = 1/BR_c \text{ for } r = 1 \tag{17.49}$$

17.7 Application of Direct Form Active R Synthesis Technique

Once the basic active R component simulators for inductors, capacitors and FDNRs in grounded as well as in floating modes are available, OA-R filters can be realized in element substitution form.

While applying the technique, selection of proper circuit simulators for a particular application is important as a large number of such circuits are available in the literature. In general, there are three aspects which need consideration while selecting component simulators: (i) complexity and component count in the final realization, (ii) sensitivity of parameters and (iii) stability.

Based on the circuit simulators discussed in the chapter so far, it can be said that all grounded elements, inductor, capacitor and FDNR, and FI use low active and passive component count, and do not require critical component matching. The FC and FDNR not only require a

https://doi.org/10.1017/9781108762632.018 Published online by Cambridge University Press

large number of components but also require semi-critical component matching. Therefore, it may be inferred that the active R immittance simulation technique is attractive when the original passive RLC network (generally ladders) either do not have FCs, or their number is small. It can be noted that, in contrast to active RC synthesis, the realization of FIs is not a problem in the OA-R case. Similarly, the FDNR approach is preferred when the original passive RLC network has a minimum of FCs and resistors, unless some better simulators for FC and floating FDNR are available.

Example 17.4: Obtain a fully OA-R filter circuit and its response for the specifications given in Example 17.2.

Solution: In Example 17.2, FIs were replaced by an OA-R simulator, but the resulting circuit was still OA-RC, though it could be used at high frequencies. The same passive ladder was realized in Example 17.3 using the FDNR technique, which is still an OA-RC one. If we want a complete OA-R circuit, both of these circuits could be used. However, in the circuit of Figure 17.9(a), we need to simulate one GC and one FC; whereas for the circuit of Figure 17.6(a), we need to simulate three GCs, in addition to two FIs. Opting for the second choice, the high-quality GC-2 of Figure 17.11(a) is employed, for which resistances are obtained using equation (17.35) with $B = 2\pi \times 10^6$ rad/s as:

$$R_{c1,5} = \frac{1+\left(2\times10^5 / 2\pi\times10^6\right)^2}{2\pi\times10^6\times8.529\times10^{-9}} = 18.67\,\Omega$$

$$R_{c3} = \frac{1+\left(2\times10^5 / 2\pi\times10^6\right)^2}{2\pi\times10^6\times12.709\times10^{-9}} = 12.53\,\Omega$$

For the two FIs having values of 6.148 mH, the required resistances will be:

$$R_{L21} = R_{L22} = R_{L41} = R_{L42} = 38.68\ \text{k}\Omega$$

The final OA-R circuit is shown in Figure 17.13(a) and the simulated response is shown in Figure 17.13(b). Pass band edge frequency is 31.88 kHz (200.4 krad/s). Its dc gain is 0.495, maximum gain is 0.501 and minimum gain in the pass band is 0.466, which corresponds to a ripple width of 0.624 dB. The obtained response is close to the design; small difference in gain value near cut-off frequencies is likely due to the non-idealness of the simulated FIs and GCs.

https://doi.org/10.1017/9781108762632.018 Published online by Cambridge University Press

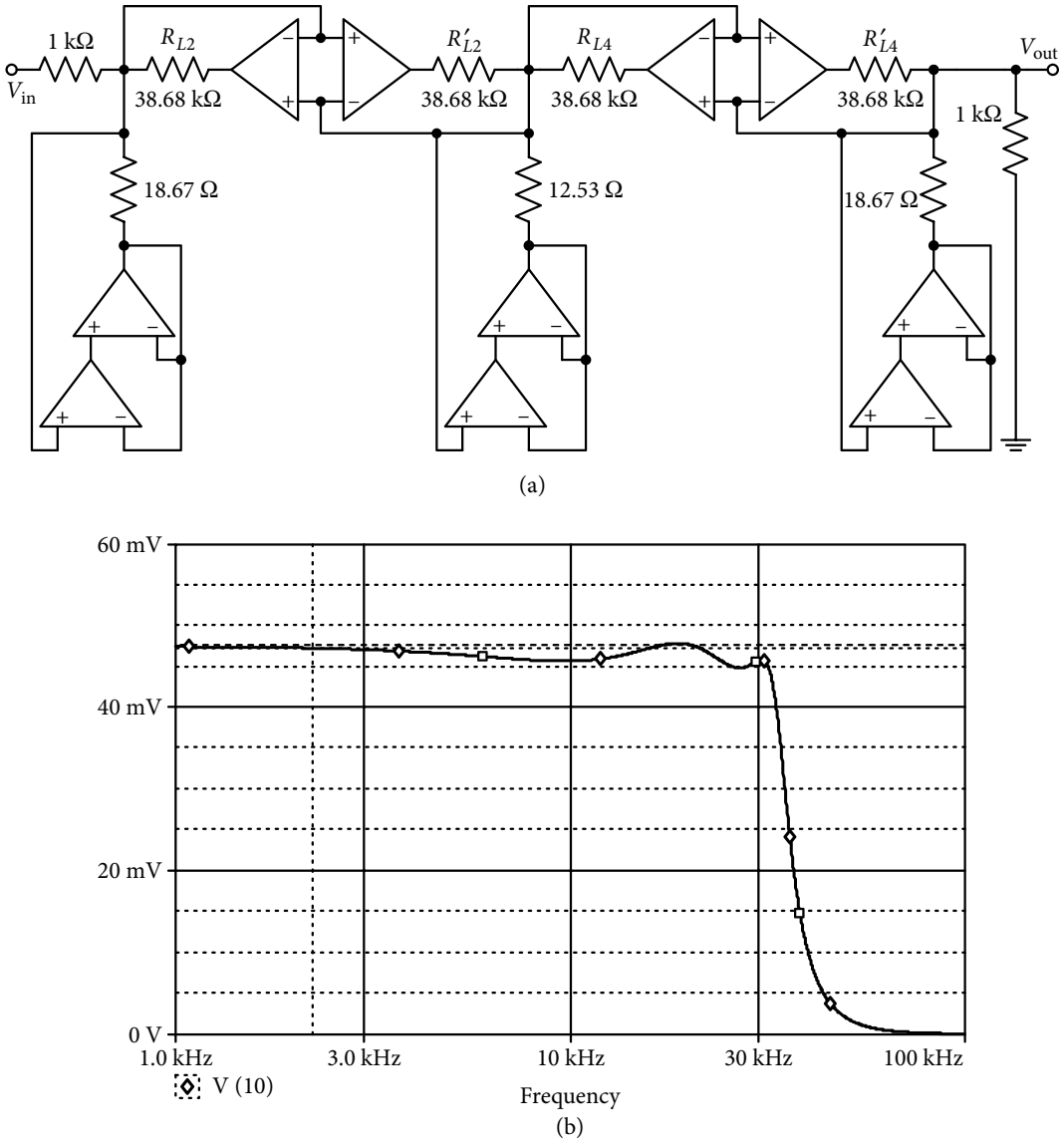

Figure 17.13 (a) Active R structure for fifth-order Chebyshev filter using immittance simulation for Example 17.4. (b) Simulated magnitude response.

17.8 Cascade Form Active R Synthesis

As mentioned in Chapter 10 and other chapters as well, in cascade form of synthesis, the nth order transfer function is realized as a non-interacting cascade of second-order section for even n, and a first/ third-order section is also included for odd n. Hence, it is necessary to develop

https://doi.org/10.1017/9781108762632.018 Published online by Cambridge University Press

and study the realization of multifunctional second-order sections, as well as first-order active R sections.

First-order Active R Circuits: A bilinear circuit for realizing active R first-order response is given in Figure 17.14(a) and the LP and HP responses are obtained from it by simply opening and/or short circuiting some resistances [17.7]. Analysis of the circuit using the approximated model of equation (17.1) gives the transfer function:

$$\frac{V_{out}}{V_{in}} = \frac{R_3\left(R_4 + R_5\right)s + B\left(R_1R_5 - R_2R_4\right)}{\left(R_1 + R_2 + R_3\right)\left(R_4 + R_5\right)s + BR_1(R_4 + R_5)} \tag{17.51}$$

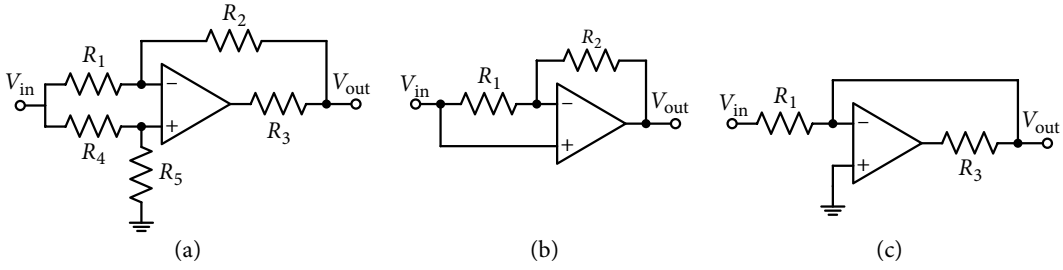

Figure 17.14 (a) A general first-order active R section; (b) low pass section obtained from (a) and (c) high pass section obtained from (a).

The circuit gives LP response if $R_3 = R_4 = 0$ and $R_5 = \infty$, as shown in Figure17.14(b). Its transfer function from equation (17.51) is:

$$\frac{V_{out}}{V_{in}} = \frac{BR_1/(R_1 + R_2)}{s + BR_1/(R_1 + R_2)} \tag{17.52}$$

HP response becomes available when $R_2 = R_5 = 0$ and $R_4 = \infty$, as shown in Figure17.14(c). Its transfer function from equation (17.51) is:

$$\frac{V_{out}}{V_{in}} = \frac{R_3}{R_1 + R_3}\left\{\frac{s}{s + R_3/(R_1 + R_3)}\right\} \tag{17.53}$$

17.9 Biquadratic Section Using Two OAs

A number of multifunctional biquadratic active R filtering sections have been made available using two or three OAs [17.8][17.9]. We will first discuss an approach for the realization of a general active R biquadratic filter; this approach uses only two OAs and resistances. By a proper adjustment of resistances, the filter is seen to realize important second-order responses. By using dual OAs on the same chip like 747, the inherently matched characteristics are utilized to advantage.

https://doi.org/10.1017/9781108762632.018 Published online by Cambridge University Press

The basic scheme is shown in Figure 17.15 [17.9]. The voltages at the inverting terminals of the OAs are expressed as a linear combination of terminal voltages V_1, V_2 and V_3 as:

$$V_4 = a_1V_1 + a_2V_2 + a_3V_3 \tag{17.54a}$$

$$V_5 = b_1V_1 + b_2V_2 + b_3V_3 \tag{17.54b}$$

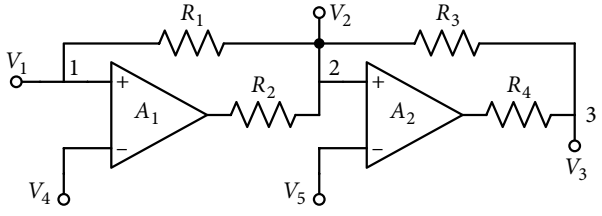

Figure 17.15 Block schematic for active R biquad realization.

The real and positive coefficients a_i' and b_i' are obtained through resistance ratios. Complete filter realization, using the scheme of Figure 17.15, is shown in Figure 17.16, where the coefficients a_i' a nd b_i', $i = 1$ to 3 are given by:

$$a_1 = \frac{R_6R_7R_8}{(\Delta R)}, a_2 = \frac{R_5R_7R_8}{(\Delta R)}, a_3 = \frac{R_5R_6R_8}{(\Delta R)} \tag{17.55}$$

$$\text{With } \Delta R = R_6R_7R_8 + R_5R_6R_7 + R_5R_7R_8 + R_5R_6R_8 \tag{17.56}$$

$$b_1 = \frac{R_{10}R_{11}R_{12}}{(\Delta R)'}, b_2 = \frac{R_9R_{11}R_{12}}{(\Delta R)'}, b_3 = \frac{R_9R_{10}R_{12}}{(\Delta R)'} \tag{17.57}$$

$$\text{With } (\Delta R)' = R_9R_{10}R_{11} + R_{10}R_{11}R_{12} + R_9R_{10}R_{12} + R_9R_{11}R_{12} \tag{17.58}$$

A little manipulation of equations (17.55) and (17.57) gives the resistance ratios:

$$\frac{R_5}{R_6} = \frac{a_2}{a_1}, \frac{R_5}{R_7} = \frac{a_3}{a_1}, \frac{R_6}{R_7} = \frac{a_3}{a_2} \tag{17.59}$$

$$\frac{R_9}{R_{10}} = \frac{b_2}{b_1}, \frac{R_9}{R_{11}} = \frac{b_3}{b_1}, \frac{R_{10}}{R_{11}} = \frac{b_3}{b_2} \tag{17.60}$$

Since the coefficients a_i' and b_i' are obtained through passive circuits, the following condition has to be satisfied.

https://doi.org/10.1017/9781108762632.018 Published online by Cambridge University Press

$$a_1 + a_2 + a_3 \le 1 \tag{17.61a}$$

$$b_1 + b_2 + b_3 \le 1 \tag{17.61b}$$

With OAs represented by approximated first-pole roll-off model, analysis of Figure 17.16 gives the following relations for pole frequency and pole-Q as:

$$\omega_o = B\left[\frac{\{a_2b_3 + a_3(1-b_2)\}G_2G_4}{(G_1+G_2)(G_3+G_4)+G_3G_4}\right]^{\frac{1}{2}} \tag{17.62}$$

$$Q = \frac{\left[\{a_2b_3 + a_3(1-b_2)\}G_2G_4\left\{(G_1+G_2)(G_3+G_4)+G_3G_4\right\}\right]^{\frac{1}{2}}}{b_3G_4(G_1+G_2+G_3)+a_2G_2(G_3+G_4)+a_3G_2G_3-(1-b_2)G_3G_4} \tag{17.63}$$

A large number of filter realizations are possible from Figure 17.16 by taking output at terminal 2 or 3. Out of this large number of possibilities, two cases are discussed here; the other cases are left as exercises.

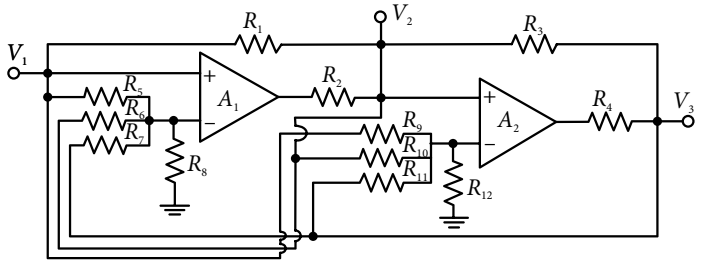

Figure 17.16 General active R biquad from Figure 17.15 with multiple feedbacks.

Case 1: In addition to other responses, BP (band pass) response becomes available when the output is taken at terminal 2. For its realization, based on the choice of feedbacks, the obtained resulting transfer function, filter parameters and design equations are given in Table 17.1.

Table 17.1 BP realization when output is taken at terminal 2 in Figure 17.16

Required conditions	Resulting transfer function	Filter parameters	Design equations
$G_1 = G_3 = 0$ $G_2 = G_4 = G$ $b_1 = b_2 = b_3 = 0$	$\dfrac{B(1-a_1)s}{s^2 + a_2Bs + a_3B^2}$	$\omega_o = B(a_3)^{\frac{1}{2}}$ $Q_o = (a_3)^{\frac{1}{2}} / a_2$ $H_o = (1-a)/a_2$	$a_1 = 1 - \omega_{on}H_o/Q_o$ $a_2 = \omega_{on}/Q_o$ $a_3 = \omega_{on}^2$

https://doi.org/10.1017/9781108762632.018 Published online by Cambridge University Press

Sensitivity figures of the general biquadratic section can be obtained using the incremental sensitivity measure discussed in Chapter 6. Sensitivities can also be found for specific filters, while assuming gain bandwidth products as B_1 and B_2. Evaluation of sensitivities of ω_o and Q_o for the BP filter gives the following values.

$$S^{\omega_o}_{G_1,G_2,G_3,G_4} = 0,\ S^{\omega_o}_{a_1,a_2} = 0,\ S^{\omega_o}_{a_3} = \frac{1}{2},\ S^{\omega_0}_{b_1,b_2,b_3} = 0,\ S^{\omega_o}_{B_1,B_2} = \frac{1}{2}$$

$$S^{Q_o}_{G_1,G_2,G_3,G_4} = 0,\ S^{Q_o}_{a_1} = 0,\ S^{\omega_o}_{a_2} = -1,\ S^{\omega_o}_{a_3} = \frac{1}{2},\ S^{Q_o}_{b_1,b_2,b_3} = 0,\ S^{\omega_o}_{B_1,B_2} = -\frac{1}{2}$$

Example 17.5: Using OAs with $B = 2\pi \times 10^6$ rad/s, design a BP filter with center frequency of 100 kHz, pole-Q = 5 and mid-band gain of 10, when the output is taken at terminal 2 in Figure 17.16.

Solution: For the second-order BPF obtained from Figure 17.16 and shown in Figure 17.17 (a), $\omega_{on} = \omega_o/B = 0.1$. Using the design equation from Table 17.1, we get:

$a_1 = 0.8$, $a_2 = 0.02$, $a_3 = 0.01$, and $b_1 = b_2 = b_3 = 0$

From equation (17.59), the resistance ratios are:

$$\frac{R_5}{R_6} = \frac{1}{40},\ \frac{R_5}{R_7} = \frac{1}{80}$$

Selecting R_5 = 3 kΩ,we get R_6 = 120 kΩ and R_7 = 240 kΩ.

From the expression of a_1 in equation (17.55), R_8 = 16.1 kΩ. The choice of $R_2 = R_4$ is arbitrary; hence, it is chosen as 3 kΩ equal to R_5.

Simulated magnitude response of the BP filter is shown in Figure 17.17(b). Center frequency is 100.23 kHz, mid-band gain is 10.122 and with a bandwidth of 19.55 kHz, the obtained value of pole-Q = 5.12; excellent results.

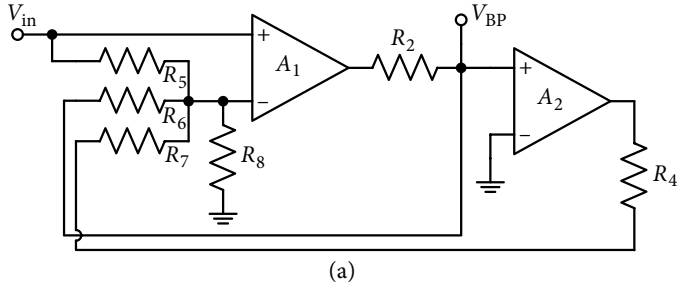

(a)

https://doi.org/10.1017/9781108762632.018 Published online by Cambridge University Press

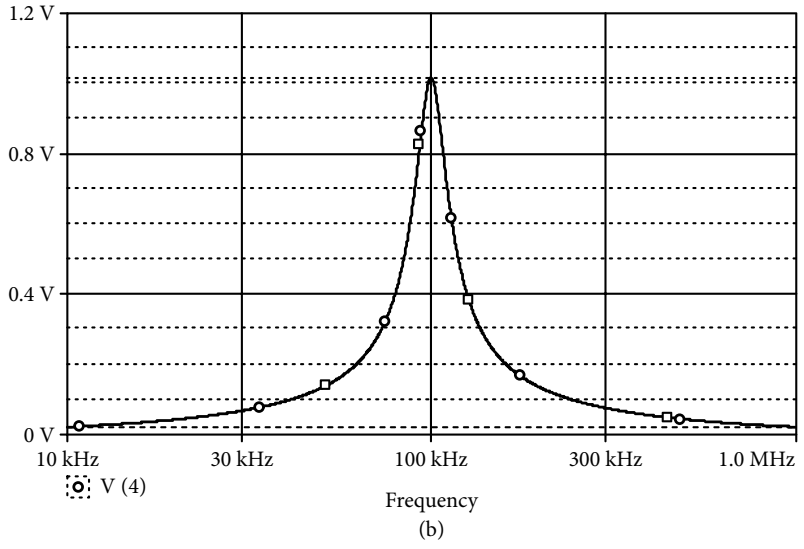

Figure 17.17 (a) Band pass section from Figure 17.16, with output taken at terminal 2, and (b) its simulated magnitude response.

Case 2: When the output is taken at terminal 3, different responses are also available. A BR (band reject) response is available with a proper choice of resistance, which is shown in Table 17.2, along with the filter parameters and design equations.

Table 17.2 Band reject realization when the output is taken at terminal 3 in Figure 17.16

Required condition	Resulting transfer function	Filter parameters	Design Equations
$G_1 = G_2 = G$ $G_3 = G_4 = G$ $a_2 = 0$ $b_1 = \frac{(2-a_1-b_2)}{3}$ $b_3 = (1-b_2)/3$	$\frac{1}{5}\frac{s^2+(1-a_1)(1-b_2)B^2}{s^2+\frac{a_3B}{5}s+\frac{a_3(1-b_2)B^2}{5}}$	$\omega_o = B\left\{\frac{a_3(1-b_2)}{5}\right\}^{1/2}$ $Q_o = \left\{\frac{5(1-b_2)}{a_3}\right\}^{1/2}$ $\omega_1 = B\{(1-a_1)(1-b_2)\}^{1/2}$	$a_1 = 1-\frac{\omega_{1n}^2}{\omega_{on}Q_o}$ $a_3 = 5\omega_{on}/Q_o$ $b_2 = 1-\omega_{on}Q_o$

Sensitivity figures of the BR filter under consideration were evaluated, which are as follows:

$$S_{G_1}^{\omega_o} = -\frac{1}{5},\ S_{G_2}^{\omega_o} = \frac{1}{10},\ S_{G_3}^{\omega_o} = -\frac{3}{10},\ S_{G_1}^{\omega_o} = -\frac{1}{5},\ S_{G_4}^{\omega_o} = \frac{1}{5},\ S_{a_1,a_2}^{\omega_o} = 0,\ S_{G_3}^{\omega_o} = \frac{1}{2},\ S_{b_1,b_2,b_3}^{\omega_o} = 0,\ S_{B_1,B_2}^{\omega_o} = \frac{1}{2}$$

$$S_{G_1}^{Q_o} = -\frac{1}{5}\left(1-\frac{Q_o^2}{3}\right),\ S_{G_2}^{Q_o} = -\frac{3}{10}\left(1-\frac{Q_o^2}{9}\right),\ S_{G_3}^{Q_o} = -\frac{7}{10}\left(1-\frac{4Q_o^2}{21}\right),\ S_{G_4}^{Q_o} = -\frac{4}{5},$$

$$S_{a_1,a_2}^{Q_o} = 0,\ S_{a_3}^{Q_o} = -\frac{1}{2},\ S_{b_1,b_2}^{Q_o} = 0,\ S_{b_3}^{Q_o} = -\frac{Q_o^2}{15},\ S_{B_1}^{Q_o} = -\frac{1}{2},\ S_{B_2}^{Q_o} = \frac{1}{2}$$

https://doi.org/10.1017/9781108762632.018 Published online by Cambridge University Press

17.10 General Biquad Using Three OAs

Some filter sections using two OAs were discussed in the last section; many more are available in the literature. Though most of the responses were possible, all types of responses are not available. The ones which are available, are with restricted independent control of the response parameters like pole-frequency, pole-Q and gain at the low, high or mid frequencies. Sometimes, design also results in high resistance spread. Moreover, when the response is taken from a terminal other than the output terminal of the OA, its performance becomes load-sensitive for cascading purpose. In such a case, an additional buffer is required, which effectively makes it a three OAs filter. It is therefore, suggested to use the well-known techniques of adding the input signal with two other responses from a two OAs filter, to obtain the general biquadratic function, as shown in Chapter 8.

17.11 Basic Techniques for Active C Synthesis

As the active C network synthesis is also an off-shoot of the active RC synthesis, like the active R case, the basic techniques remain the same.

While employing direct form synthesis in the active R or active RC filters, the starting point is an RLC prototype network; most often the doubly terminated ladder. Same approach is used in the case of direct form of active C filters; the final network would contain only OAs and capacitors.

Discussion on the cascade form of the active C synthesis begins in Section 17.14. Its basic steps are the same, that is, cascading non-interactive second-order sections (Section 17.15) and a first- or third-order section, if needed. Hence, efforts will be made to get active C sections which have low component sensitivities, wide frequency range tunability, and high functional versatility. Low and medium Q filters are realized and examples of OA-C cascade design are shown in Section 17.16. Both active R and active C filters have practical limitations on account of the dependence of their parameters on the gain bandwidth product of the OAs employed. These limitations and some methods to minimize these limitations are briefly discussed in Section 17.17.

17.12 Active OA-C Simulation of Immittance Functions

This section is primarily concerned with the OA-C simulation of important types of immittance functions. The basic object of these simulations is to use them in the active C direct form synthesis for the realization in MOS (metal–oxide semiconductor)-compatible circuits.

Realization of Active C Inductors: Inductors can be realized in the ideal form, as well as in non-ideal form. Generally, ideal form realization requires a greater number of components and need some matching of components but may give better performance when employed in a filter circuit; though real comparison can be done only after their usage. Figure 17.18(a) shows

https://doi.org/10.1017/9781108762632.018 Published online by Cambridge University Press

the circuit realization of an ideal GI. Employing OA model of equation (17.1), analysis of the circuit in Figure 17.18(a) gives the driving point impedance as:

$$Z(s)=\frac{1}{sC}\frac{\left(B_2-B_3\right)s^4-\left(B_2-B_3\right)B_4B_5s^2+B_2B_3B_4s^2}{\left(B_2-B_3\right)s^4-\left(B_2-B_3\right)B_4B_5s^2-\left(B_1-B_4\right)B_2B_3s^2+B_1B_2B_3B_4B_5} \tag{17.64}$$

In equation (17.64), if $B_1 = B_4$ and $B_2 = B_3$, then the expression of impedance simplifies as:

$$Z(s) = s/(CB_1\,B_5) = sL_e \tag{17.65}$$

Expression in equation (17.65) represents an ideal inductance, shown in Figure 17.18(b).

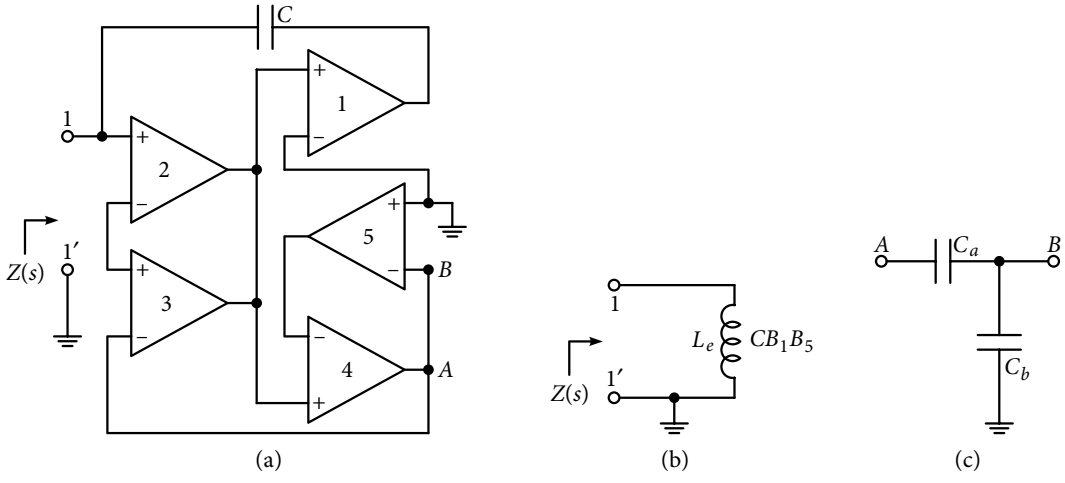

Figure 17.18 (a) Ideal OA-C inductance simulator; (b) simulated ideal inductor when $B_1 = B_4$ and $B_2 = B_3$, and (c) a capacitive attenuator.

Realization of the ideal inductor requires matching of two pairs of matched OAs in Figure 17.18 (a), which is not difficult to achieve when OAs are fabricated on the same chip like the LM 747, or while integrating the entire circuit on a chip and placed close by.

Value of the inductance can be tuned with C and B_5, without affecting the condition of the required matching of $B_1 = B_4$ and $B_2 = B_3$.

Realized value of the inductance can be enhanced by a factor $k = (1 + C_b/C_a)$, by inserting the capacitive attenuator of Figure 17.18(c) between points A and B of the inductor circuit in Figure 17.18(a). The attenuator affects the effective value of B_5 and realizes inductance value as:

$$L_e' = \frac{1}{CB_1(B_5 / k)} = kL_e \tag{17.66}$$

https://doi.org/10.1017/9781108762632.018 Published online by Cambridge University Press

A large number of non-ideal inductors have been realized [17.10] in which parasitic resistance and capacitance appear in series or parallel form. One such circuit is shown in Figure 17.19(a) for which the following driving point admittance is obtained.

$$Y(s) = B_1C_1 + s(C_1 + C_2) + (B_1B_2C_2 / s) \rightarrow \frac{1}{R_e} + sC_e + \frac{1}{sL_e} \tag{17.68}$$

Equation (17.68) represents a parallel combination of resistance and capacitance with the realized GI, with the following expressions as shown in Figure 17.19(b):

$$R_e = 1/(B_1\ C_1),\ C_e = (C_1 + C_2) \text{ and } L_e = 1/(B_1B_2C_1) \tag{17.69}$$

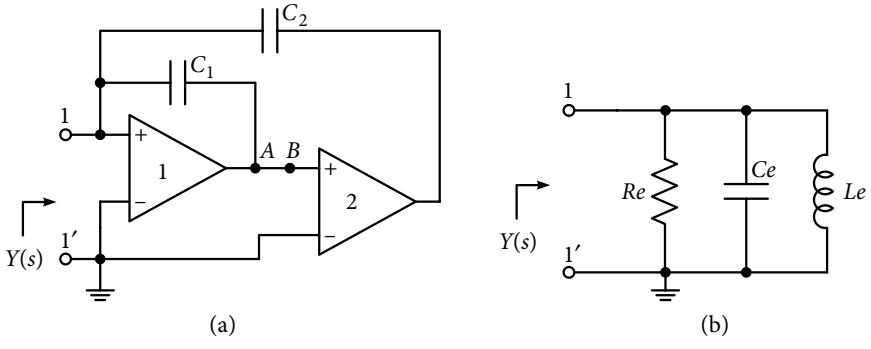

Figure 17.19 (a) An RLC simulator and (b) its equivalent representation.

Though the circuit simulates a parallel combination of R, L and C, it employs only two OAs and two capacitors compared to the five OAs and one capacitor needed in the realization of an ideal GI. In addition, the circuit does not require any matching constraint and presents a fairly good flexibility in the design of R, L and C parameters. The sensitivity figures of the circuit are less than or equal to unity in magnitude as shown here.

$$S^{R_e}_{B_2,C_2} = 0, S^{R_e}_{B_1,C_1} = -1, S^{C_e}_{B_1,B_2} = 0, S^{C_e}_{C_1,C_2} = \frac{C_1}{C_1 + C_2}, S^{L_e}_{C_1} = 0, S^{L_e}_{B_1,B_2,C_2} = -1$$

Realization of Active C FDNRs: Many circuits have been made available for the realization of ideal and non-ideal FDNR in reference [17.10]. One such non-ideal FDNR simulators is shown in Figure 17.20(a). Its admittance function is found as:

$$Y(s) = sC + 1/\left(\frac{1}{CB_1} + \frac{B_2}{s^2C}\right) = sC_e + 1/\left(R + \frac{1}{s^2D}\right) \tag{17.70}$$

Equation (17.70) shows that the circuit realizes a non-ideal FDNR, having parasitic resistance and capacitance, which are shown in Figure 17.20(b). Expressions of the realized grounded

https://doi.org/10.1017/9781108762632.018 Published online by Cambridge University Press

FDNR, its parasitic elements and the enhanced value FDNR after introducing capacitive attenuators are:

$$D = C/B_2,\ C_e = C,\ R = 1/CB_1 \text{ and } D' = kD \tag{17.71}$$

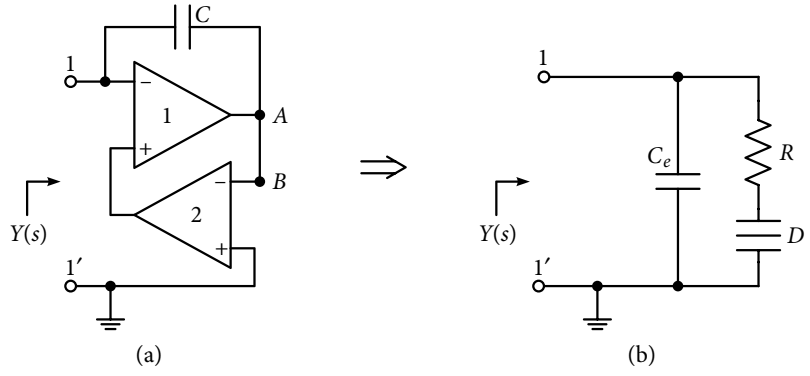

Figure 17.20 (a) Parallel C: (R, D) simulator and (b) its equivalent circuit.

These expressions for C, R and D parameters indicate a convenient and flexible design over a fairly wide range, and the realization of the circuit does not require any matching of bandwidth of OAs. Again, enhancement in the D value and its easy passive and active tuning is possible by connecting a capacitive attenuator of Figure 17.18(c) between terminals A and B in Figure 17.20 (a); incremental sensitivity values are also low, being less than or equal to unity.

Realization of Active C FDNCs: Frequency dependent negative capacitance (FDNC) is an unconventional and relatively less used element [17.11]. The s^2 transformation on a capacitor C, as shown in Figure 17.21(a), yields the following admittance function:

$$Y(s) = s^3 F \tag{17.72}$$

In equation (17.72), F is a real positive constant, and for $s = j\omega$, we get:

$$Y(j\omega) = -j\omega^3 F \tag{17.73}$$

Hence, the circuit element shows the characteristics of a frequency dependent negative capacitor.

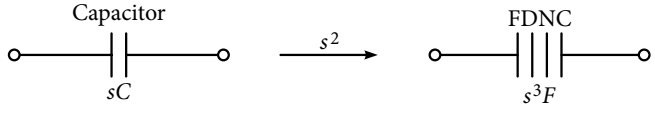

Figure 17.21 Frequency transformation applied to obtain FDNC from a capacitor.

https://doi.org/10.1017/9781108762632.018 Published online by Cambridge University Press

A non-ideal FDNC-based circuit realization is shown in Figure 17.22, along with its equivalent circuit. Its analysis gives the driving point impedance function as:

$$Z(s)=\frac{C_{1-2}}{sC_1C_2}+\frac{1}{\frac{s^2C_1C_3}{B_1C_4}+\frac{s^3C_1C_{3-4}}{B_1B_2C_4}}=\frac{1}{sC_e}+\frac{1}{s^2D+s^3F} \tag{17.74}$$

In equation (17.74), $C_{i-j} = C_i + C_j$ (the symbol will be used later as well), and elements of the equivalent circuit are expressed as:

$$C_e=\frac{C_1C_2}{C_{1-2}},\ D=\frac{C_1C_3}{B_1C_4}\text{ and }F=\frac{C_1C_{3-4}}{B_1B_2C_4} \tag{17.75}$$

The non-ideal FDNC is economical from the point of element use and does not require any component matching. As expressed in equation (17.75) circuit in Figure 17.22 simulates a series combination of a capacitor C_e with a parallel D: F impedance function. The D and F parameters are controllable with B_1 and B_2.

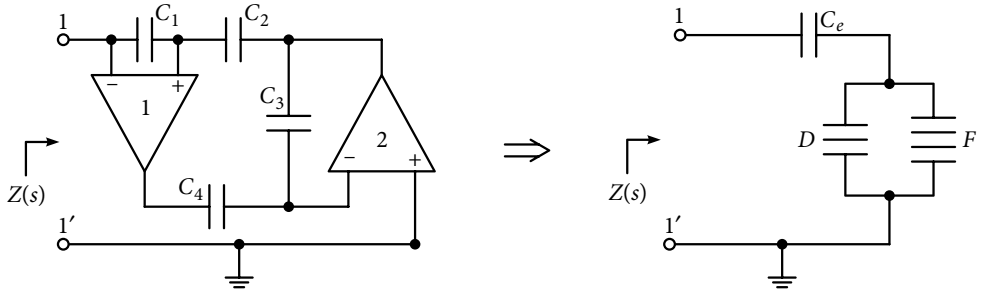

Figure 17.22 Series C: (D||F) simulator and its equivalent representation.

Realization of Active C Resistors: In addition to the requirements of simulating inductance, FDNR and FDNC, sometimes resistances are also to be simulated in terms of OAs and capacitors; two such circuits are discussed in brief.

In addition to the simulation of an ideal resistor, some other useful immittances have been obtained. For example, circuit analysis for Figure 17.23 gives the driving point admittance as:

$$Y(s)=sC\frac{s^2(B_3-B_2)+sB_2B_3}{s^2(B_3-B_2)-B_1B_2B_3}$$

$$=-s^2\,(C/B_1)=-s^2D \text{ with } B_3=B_2 \tag{17.76}$$

Equation (17.76) implies that under matching conditions, it realizes a frequency dependent positive resistance (FDPR), as for $s = j\omega$, $Y(j\omega) = \omega^2 D$.

https://doi.org/10.1017/9781108762632.018 Published online by Cambridge University Press

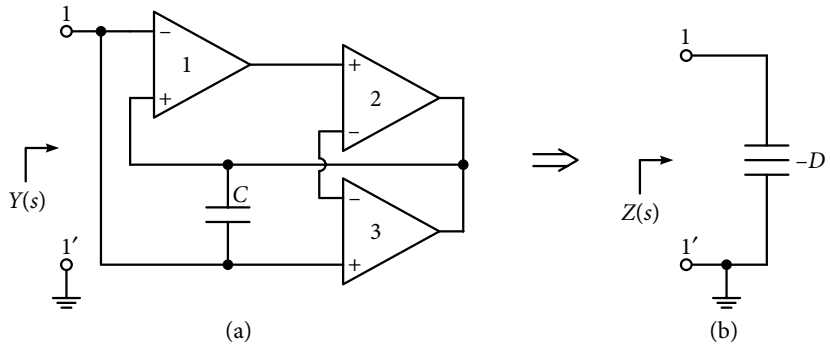

Figure 17.23 Ideal OA-C FDPR and its equivalent circuit when $B_2 = B_3$.

Another useful circuit shown in Figure 17.24 uses only one OA and a capacitor and realizes a parallel combination of a resistance and a capacitor as obtainable from the following driving point admittance function:

$$Y(s) = CB + sC \rightarrow (1/R) + sC_e \tag{17.77}$$

The circuit needs no matching; hence, sensitivity is always low. The circuit also realizes a parallel combination of same value components, but the resistance becomes negative, if the input terminals of the OA are interchanged.

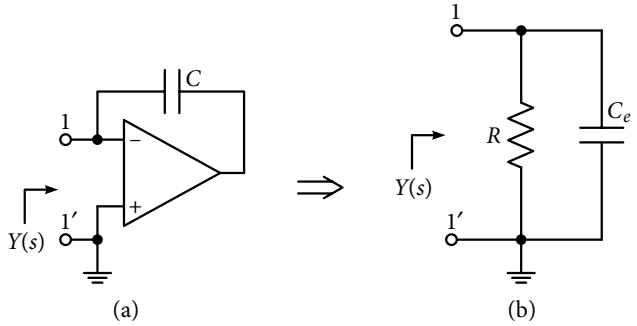

Figure 17.24 Parallel R:C simulator and its equivalent circuit.

Simulation of Floating Components: A floating parallel LC simulator is described in this section using the back-to-back parallel technique [17.2]. The BBB (basic building block) for the realization is shown in Figure 17.25(a). The non-inverting terminal of the OA1 is ungrounded, and the floating form is realized by inter-connecting the two identical BBBs in a back-to-back manner, as shown in Figure 17.25(b). Routine analysis of the circuit yields the admittance matrix:

$$Y(s) = \begin{bmatrix} sC(1 + A_1A_2) & -sCA_1A_2 \\ -sC'A_1'A_2' & sC'(1 + A_1'A_2') \end{bmatrix} \tag{17.78}$$

https://doi.org/10.1017/9781108762632.018 Published online by Cambridge University Press

When BBBs are identical with: $C = C'$, $A_1 = A_1', A_2 = A_2'$ and the OAs are represented by the approximate model, equation (17.78) will modify in the frequency range $\omega^2 \lll B_1 B_2$ as:

$$Y(s) = \left(sC_e + \frac{1}{sL_e} \right) \begin{bmatrix} 1 & -1 \\ -1 & 1 \end{bmatrix} \tag{17.79}$$

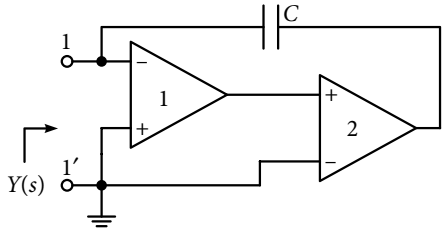

(a)

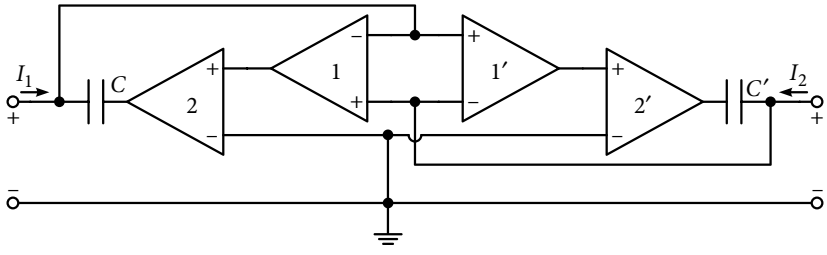

(b)

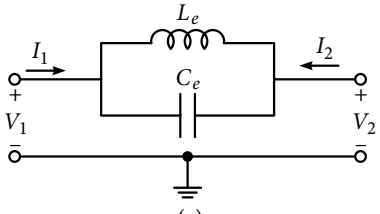

(c)

Figure 17.25 (a) Grounded parallel L:C simulator, (b) parallel L:C floating immittance simulator with back-to-back parallel technique and (c) equivalent circuit of the FI simulator.

Equation (17.79) satisfies the condition for the floating components of the parallel LC simulator, viz., $y_{11} = -y_{12} = -y_{21} = y_{22}$ [17.12], which is shown in Figure 17.25(c). Parameters of the realized equivalent circuit are given as:

$$C_e = C \text{ and } L_e = 1/(B_1 B_2 C) \tag{17.80}$$

The parameters are identical to those for the corresponding grounded simulator from which the circuit has been derived.

https://doi.org/10.1017/9781108762632.018 Published online by Cambridge University Press

17.13 OA-C Filters: Direct Form Synthesis

In the present case, direct form synthesis approach implies realization of first-, second-, and higher-order OA-C filters. The synthesis technique aims to realize the final network in a form suitable for micro miniaturization in MOS technology [17.13].

The following three techniques are proposed [17.14]: Inductance-based approach; FDNR-based approach; and FDNCAP-based approach. As in earlier cases, the direct form synthesis starts with the prototype passive network whose elements are to be simulated so that the final realization contains OAs and capacitors. The choice of a particular technique will largely depend on the configuration of the prototype.

FDNR Based OA-C Filters: The FDNR approach has been used in OA-RC and active R cases and does not need any further explanation. The designer needs simulators for FDNR and resistors. However, there are two choices for the selection of simulators. Circuits simulating ideal FDNRs with ideal resistor simulator can be used. Otherwise, a clever combination of non-ideal FDNR simulators can be used. It has been observed that the latter choice results in a smaller component count and requires lesser component matching. Hence, using a non-ideal FDNR simulator, the synthesis approach is illustrated with the following examples.

A prototype second-order BE (band elimination) filter is shown in Figure 17.26(a) and its transformed FDNR version is shown in Figure 17.26(b) [17.14]. To realize the circuit in OA-C form, the non-ideal FDNR simulator of Figure 17.20(a) is used in the direct simulation of the entire shunt branch (shown within the dotted line) of the transformed circuit. It is to be noted that a capacitive potential divider in the form of C2 and C3 is connected between terminal A and B of Figure 17.20(a). Final realization of the circuit in active C form is shown in Figure 17.26(c). Modeling OA by equation (17.1), gives the transfer function as:

$$H_{\mathrm{BE}}(s)=\frac{V_{\mathrm{BE}}}{V_{\mathrm{in}}}=h_{\mathrm{BE}}\frac{s^2+\omega_n^2}{s^2+(\omega_o/Q)s+\omega_o^2}=\frac{N(s)}{D(s)} \tag{17.81}$$

$$\text{where, } h_{\mathrm{BE}}=\frac{C_0}{C_{0-1}},\ \omega_o=\omega_n=\left(B_1B_2\frac{C_2}{C_{2-3}}\right)^{0.5} \text{ and } Q=\left(1+\frac{C_0}{C_1}\right)\left(\frac{B_2}{B_1}\frac{C_2}{C_{2-3}}\right)^{0.5} \tag{17.82}$$

It is to be noted that all the parameters of the second-order filter are dependent on capacitor ratios. Incidentally, the circuit also provides BP and LP responses at the output of OA1 and OA2, respectively, and transfer functions of these responses are:

$$H_{\mathrm{BP}}(s)=\frac{\mathrm{V_{BP}}}{V_{\mathrm{in}}}=h_{\mathrm{BP}}\frac{(\omega_o/Q)s}{s^2+(\omega_o/Q)s+\omega_o^2} \tag{17.83}$$

$$H_{\mathrm{LP}}(s)=\frac{V_{\mathrm{LP}}}{V_{\mathrm{in}}}=h_{\mathrm{LP}}\frac{\omega_o^2}{s^2+(\omega_o/Q)s+\omega_o^2} \tag{17.84}$$

$$\text{where, } h_{\mathrm{BP}}=-\frac{C_0}{C_1},\ \text{and } h_{\mathrm{LP}}=\frac{C_0}{C_{0-1}} \tag{17.85}$$

https://doi.org/10.1017/9781108762632.018 Published online by Cambridge University Press

The circuit possess independent bias-voltage tuning of pole frequency $\omega_o = \omega_n$. Moreover, independent passive tuning of pole-Q is possible with C_o and /or C_1. Sensitivity figures of the filter parameters are found to be less than unity in magnitude.

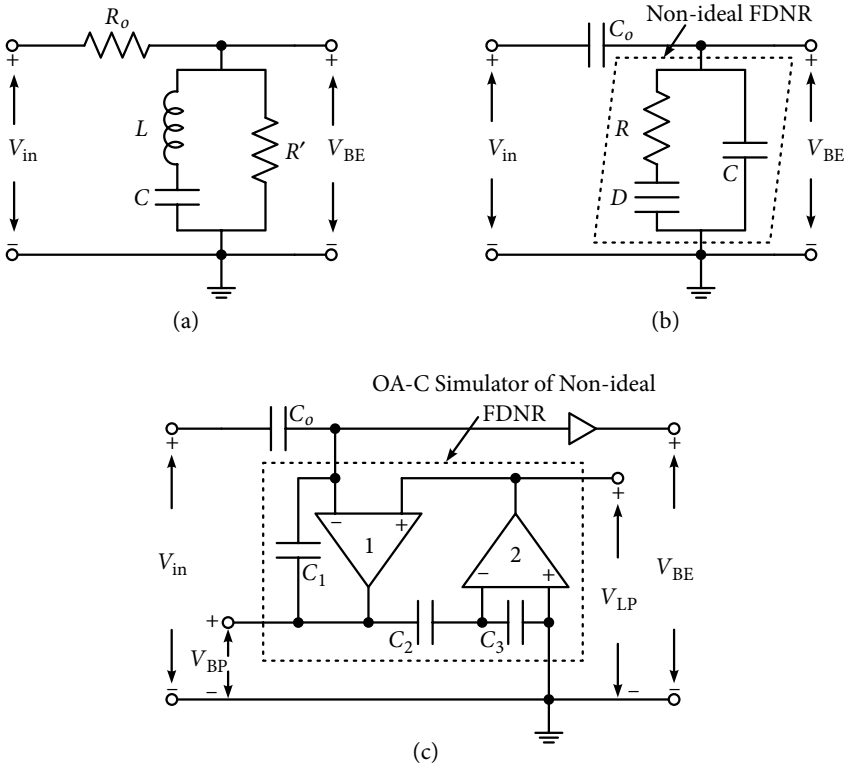

Figure 17.26 (a) Prototype-RLC band elimination filter, (b) its frequency scaled version and (c) OA-C version using non-ideal FDNR simulator.

Example 17.6: Design and test a BE filter using the circuit of Figure 17.26(c), having a notch frequency of 50 kHz and $Q = 5$. Also, find other responses available from the circuit.

Solution: In a practical circuit, values of the bandwidth of the individual OAs have to be found out or estimated according to the fabrication process used. However, in this chapter, a fixed value of $B = 2\pi 10^6$ rad/s is used for the 741 types of OAs. Using equation (17.82), ratio (C_2/C_{2-3}) will be 1/400 that will yield the ratio C_o/C_1 as 99; hence, the selected values of the capacitances are:

$$C_o = 99 \text{ pF}, C_1 = 1 \text{ pF}, C_2 = 20 \text{ pF and } C_3 = 7.98 \text{ nF} \tag{17.86}$$

To enable the flow of bias current in all OAs, 10 MΩ resistance were to be connected across C_o and C_2 in Figure 17.26(c). Simulated response of the BE and BP is shown in Figure 17.27(a).

https://doi.org/10.1017/9781108762632.018 Published online by Cambridge University Press

Simulated notch frequency, as well as center frequency of the BP is 49.776 kHz. Bandwidth of the BP response is 7.853 kHz, resulting in $Q = 6.337$ and mid-band gain is 125 (theoretical value is 99), whereas the BE filter gain at low frequencies is 0.99 and unity at high frequency. LP response is also shown in Figure 17.27(b) having unity gain at dc and peak gain of 6.28 at 49.57 kHz. Slight tuning in terms of changing C to 1.21 pF from 1 pF, increases bandwidth to 9.918 kHz, resulting in the value of Q as 5.016, mid-band gain becomes 99 for the BPF, and the peak gain of the LP response is the near theoretical value of 5 as shown in Figure 17.27(b).

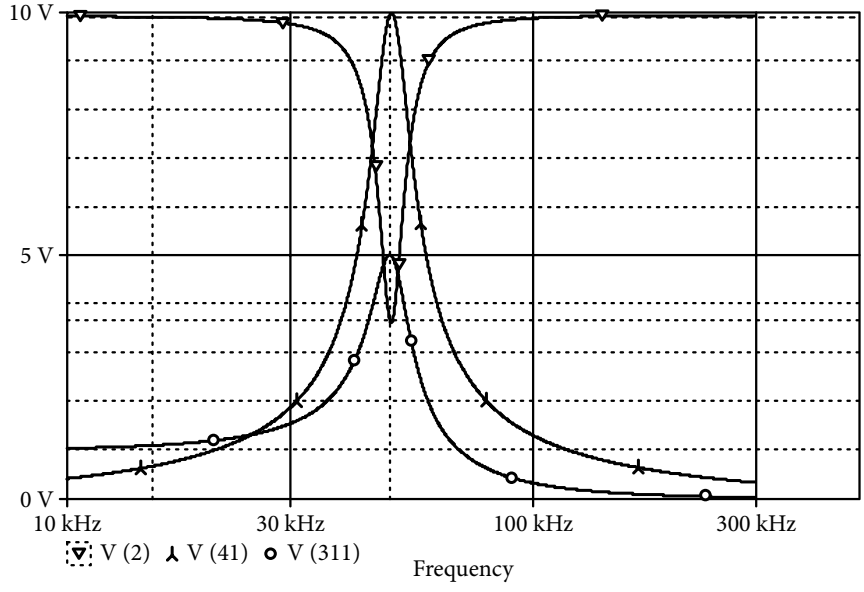

Figure 17.27 (a) Band elimination, band pass and low pass second-order responses of the circuit in Figure 17.26(c).

Inductance Simulation Based OA-C Filters: In the inductance-based approach, resistances and inductances of the prototype filter are simulated in the OA-C form and substituted in it. A passive prototype second-order HP section is shown in Figure 17.28(a). For obtaining its OA-C version, the RLC circuit is directly replaced by a non-ideal GI simulator. The simulator is shown inside the dotted line in Figure 17.28(b), which yields a parallel combination of a resistor, a capacitor and an inductor which is shown in the dotted line in Figure 17.28(a). Analysis of the circuit in Figure 17.28(b) gives the transfer function as:

$$H_{\mathrm{HP}}(s) = \frac{V_{\mathrm{HP}}}{V_{\mathrm{in}}} = \frac{h_{\mathrm{HP}} s^2}{s^2 + (\omega_o / Q)s + \omega_o^2} \tag{17.87}$$

$$\text{where, } h_{\mathrm{HP}} = \frac{C_0}{C_{0-1}},\ \omega_o^2 = B_1 B_2 \frac{C_2}{C_{0-1-2}} \frac{C_3}{C_{3-4}},\ Q = \frac{C_2}{C_1}\left(\frac{B_1}{B_2}\frac{C_{0-1-2}}{C_2}\frac{C_3}{C_{3-4}}\right)^{0.5} \tag{17.88}$$

https://doi.org/10.1017/9781108762632.018 Published online by Cambridge University Press

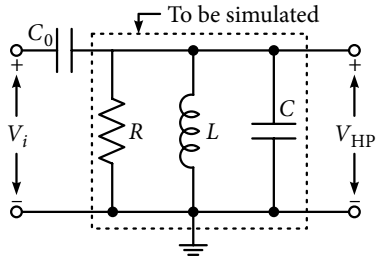

(a)

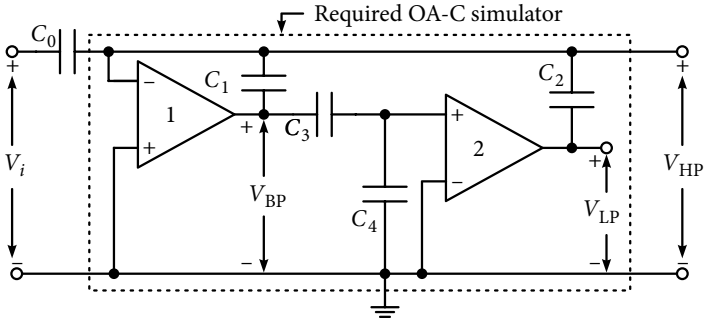

(b)

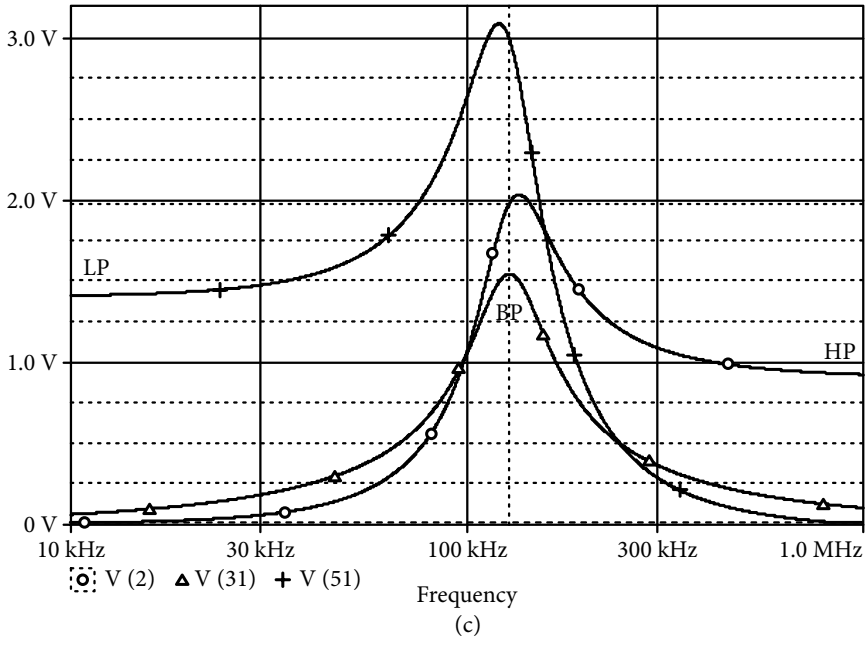

(c)

Figure 17.28 (a) Prototype passive high pass filter and (b) its OA-C version employing a non-ideal grounded inductance simulator. (c) High pass along with band pass and low pass response for Example 17.7.

https://doi.org/10.1017/9781108762632.018 Published online by Cambridge University Press

In addition to the LP response, the circuit also gives BP and LP responses as shown in Figure 17.28(b). Expressions for gain of the BP and the LP, the frequency ω_o and Q remaining the same, are:

$$h_{BP} = -(C_0/C_1);\ h_{LP} = -(C_0/C_2) \tag{17.89}$$

It is observed that filter parameters are in terms of capacitor ratios. Sensitivity figures of the filter parameters, with respect to active and passive elements, are equal or less than unity in magnitude. To provide biasing, high valued resistances are required across the capacitors C_2 and C_3.

Example 17.7: Design a second-order HP filter having 3 dB frequency of 125 kHz and $Q = 2$ using inductance simulation approach.

Solution: Use of gain bandwidth value for 741 type OAs, $B = 2\pi\,(10)^6$ rad/s, equation (17.88) gives the following values for the required capacitors.

$$C_0 = 14 \text{ nF},\ C_1 = C_2 = 1 \text{ nF},\ C_3 = 1 \text{ nF, and } C_4 = 3 \text{ nF}$$

Simulated responses of the HP along with the BP and LP are shown in Figure 17.28(c) (however, with modified value of $C_1 = 1.45$ nF for adjusting the maximum gain of the HP filter as 2). For the designed 3 dB frequency of 125 kHz, peak gain of 2.02 for the HP response occurs at 134.45 kHz, which corresponds to the simulated 3 dB frequency of 125.76 kHz. Center frequency of the BP is obtained at 127.05 kHz; bandwidth of 59.45 kHz gives $Q = 2.013$. In the case of LP, peak gain of 3.04 occurs at 120.78 kHz, resulting in the 3 dB frequency of 124.28 kHz.

FDNC Based OA-C Filters: In this approach, the passive RLC prototype network is transformed by scaling its each admittance by s^2 as shown in Figure 17.29. The resulting network N' is obtained by converting a resistor to an FDNR, an inductor to a capacitor and a capacitor to an FDNC. The FDNC has impedance of the form $(1/s^3)$ F, where F is the parameter of the element. FDNR and FDNC are then replaced by OA-C simulators. The technique is seen to be very useful in the realization of OA-C versions of those structures which have excessive number of inductances. In this approach as well, realizations using non-ideal FDNC simulators are preferred over ideal simulators. Realization of a second-order LP filter will illustrate the use of FDNC.

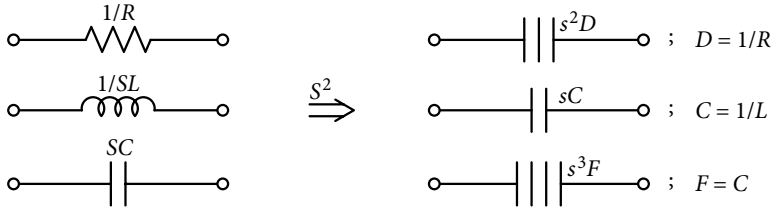

Figure 17.29 Transformation of RLC elements to DCF version by s^2 scaling on each admittance.

https://doi.org/10.1017/9781108762632.018 Published online by Cambridge University Press

Figure 17.30(a) shows a prototype second-order LP filter, and its s^2 scaled version is shown in Figure 17.30(b). It can be observed that the transformed network may be completely simulated by the FDNC based network of Figure 17.22 by taking the responses at the output of OA2 as shown in Figure 17.30(c) where capacitor C is split as parallel combination of capacitors C_1 and C_2. Analysis of the circuit yields the transfer function as:

$$H_{\mathrm{LP}}(s)=\frac{V_{\mathrm{LP}}}{V_{\mathrm{in}}}=\frac{h_{\mathrm{LP}}\omega_o^2}{s^2+(\omega_o/Q)s+\omega_o^2} \tag{17.90a}$$

$$\text{where, } h_{\mathrm{LP}}=1,\ \omega_o^2=B_1B_2\frac{C_2}{C_{1-2}}\frac{C_4}{C_{3-4}},\ \text{and } Q=\frac{C_2}{C_1}\frac{C_{3-4}}{C3}\left(\frac{B_1}{B_2}\frac{C_2}{C_{1-2}}\frac{C_4}{C_3}\right)^{0.5} \tag{17.90b}$$

Parameters of the filter are in terms of capacitor ratios, and their sensitivity figures are also low. In order to provide dc biasing, high value resistors are required across C_2 and C_3.

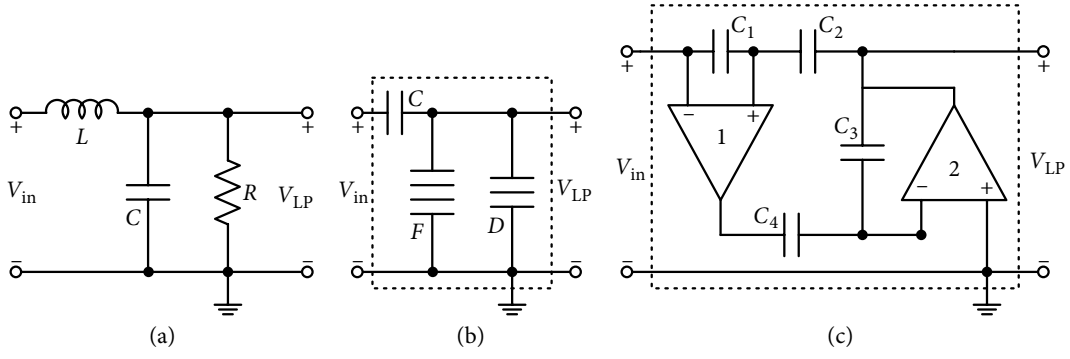

Figure 17.30 (a) Prototype RLC low pass filter, (b) its FDNC transformation, and (c) OA-C version.

17.14 OA-C Filters: Cascade Approach

The basic realization approach remaining the same, it is the second-order section, which forms the basic function to be realized, in addition, to the first-order section. When realized in OA-C form, the performance criteria remain the same which need not be repeated here.

First-order OA-C Sections: Three types of first-order circuits are studied here; LP, HP, and AP [17.15]. Figure 17.31 shows the two first-order LP sections; part (a) realizes the non-inverting section and part (b) realizes the inverting section. The transfer function for the circuit in Figure 17.31(a) will be:

$$H_1(s)=\frac{\alpha B}{s+\alpha B} \tag{17.91}$$

https://doi.org/10.1017/9781108762632.018 Published online by Cambridge University Press

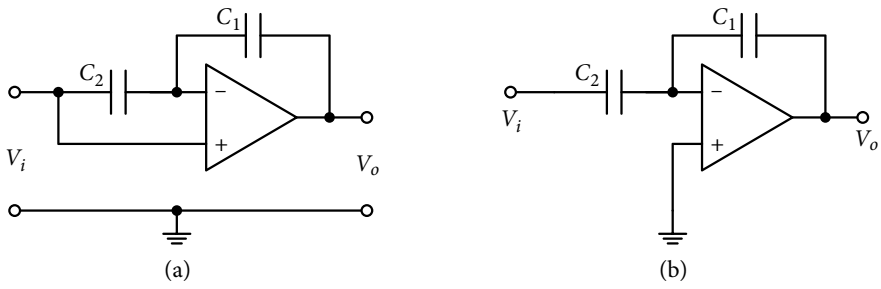

Figure 17.31 (a) Non-inverting and (b) inverting first-order low pass OA-C sections.

In equation (17.91), $\alpha = C_1/C_{1-2}$ and dc gain of the section is unity. For the inverting section shown in Figure 17.31(b), dc gain is (C_1/C_2) and the transfer function is as follows:

$$H_{11}(s) = -\frac{(1-\alpha)B}{s+\alpha B} \tag{17.92}$$

The circuit shown in Figure 17.32(a), realizes an HP section, for which transfer function is obtained as:

$$H_{12}(s) = \frac{(1-\alpha)s}{s+\alpha B} \tag{17.93}$$

Its high frequency gain will be $(1 - \alpha)$.

For the circuit shown in Figure 17.32(b), the obtained transfer function is:

$$H(s) = \frac{1}{1+\alpha_2}\frac{s-(\alpha_1\alpha_2-1)\{B/(1+\alpha_1)\}}{s+\{B/(1+\alpha_1)\}} \tag{17.94}$$

where, $\alpha_1 = C_1/C_2$, and $\alpha_2 = C_3/C_4$. (17.95)

For $\alpha_1\alpha_2 - 1 = 1$ or $\alpha_1\alpha_2 = 2$, the circuit realizes the following AP function:

$$H_{AP}(s) = \frac{1}{(1+\alpha_2)}\frac{s-\{B/(1+\alpha_1)\}}{s+\{B/(1+\alpha_1)\}} \tag{17.96}$$

When the circuit is used as a phase shifter, its magnitude and phase shift are given as:

$$|H_{AP}(j\omega)| = \frac{1}{(1+\alpha_2)} \text{ and } \varphi = \pi - 2\tan^{-1}\left\{\frac{(1+\alpha_1)\omega}{B}\right\} \tag{17.97}$$

All the parameters of the first-order sections are in terms of capacitor ratios; sensitivity figures of all the parameters are also small being equal to or less than unity in magnitude. To provide the bias current, a high value resistance is to be connected across capacitor C_1 in HP and LP cases.

https://doi.org/10.1017/9781108762632.018 Published online by Cambridge University Press

Example 17.8: Design a first-order LP and HP filter in OA-C form having a 3 dB frequency of 50 kHz.

Solution: For the LP filter of Figure 17.31(a) for the 741 type OA, with (ω_o/B) = (50/1000), $\alpha = C_1/C_{1-2}$ = 1/20. Hence, for a selected value of C_1 = 0.1 nF, C_2 = 1.9 nF. Similarly, for the HP filter of Figure 17.32(a), for the same cut-off frequency C_1 = 0.1 nF and C_2 = 1.9 nF. Simulated responses of the LP and HP are shown in Figure 17.32(c). Cut-off frequency for the LP response is 51.2 kHz and dc gain is unity. For the HP case, cut-off frequency is 50.7 kHz and high frequency gain is 0.973 against 0.95.

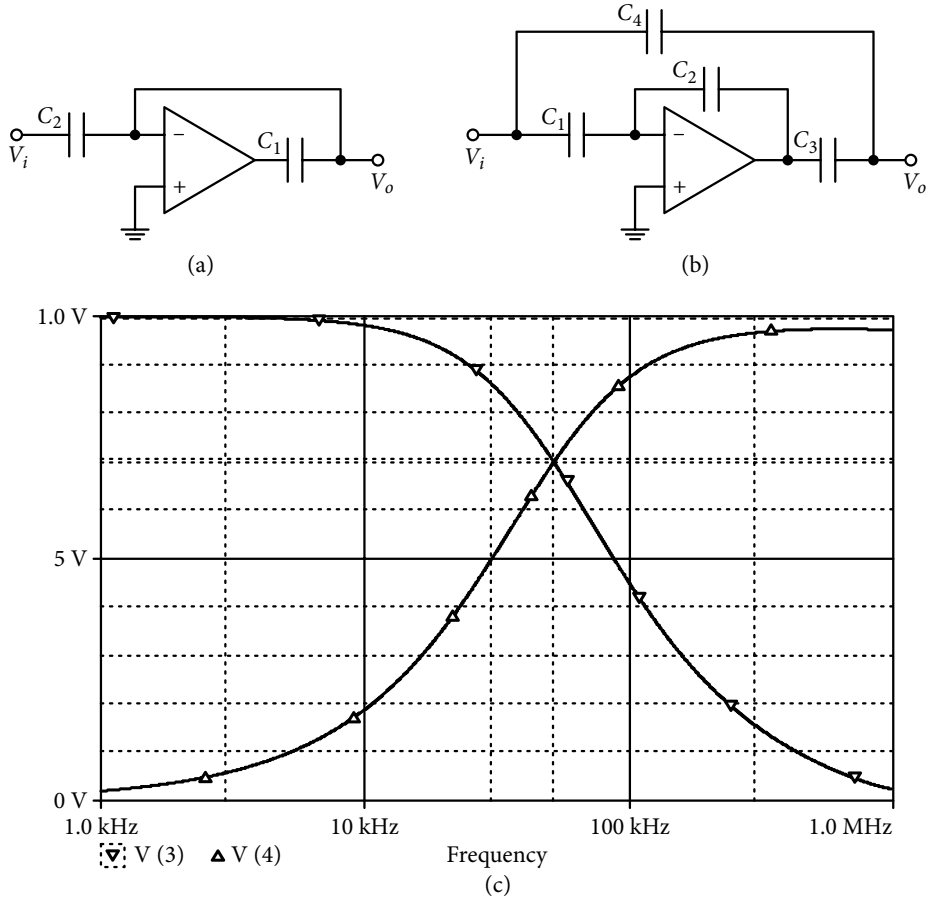

Figure 17.32 First-order (a) high pass and (b) an all pass OA-C sections. (c) Responses of the first-order low pass and high pass filters of Figure 17.31 and 17.32(a).

17.15 Second-order OA-C Filters

In this section, two circuits for the realization of low to medium Q filters, and two circuits for medium to high Q filters are discussed [17.16]. Only OAs and capacitor ratios are employed in

https://doi.org/10.1017/9781108762632.018 Published online by Cambridge University Press

all the configurations. These circuits simultaneously realize LP and BP responses at the output of the OAs. These may therefore, constitute the non-interactive basic building blocks for the realization of higher-order filters.

Low to Medium *Q* Filters Two multifunctional OA-C filters for the realization of LP and BP responses are shown in Figure 17.33(a) and (b). The expressions for the voltage transfer functions are given in Table 17.3, where $\alpha_1 = C_1/C_{1-2}$, and $\alpha_2 = C_3/C_{3-4}$.

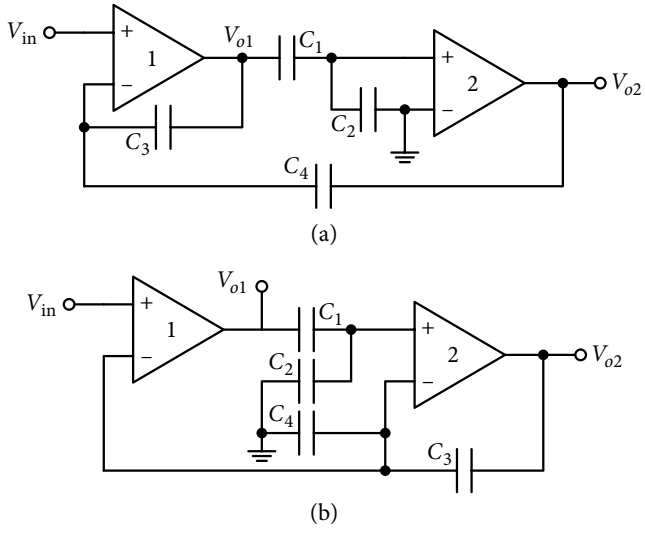

Figure 17.33 Low to medium-*Q* low pass and band pass second-order filters.

Table 17.3 Voltage ratio transfer functions of the filters of Figure 17.33(a) and (b)

Fig. No.	H_{BP}	H_{LP}
17.33(a)	$\frac{V_{o1}}{V_{in}} = \frac{sB_1}{s^2 + sB_1\alpha_2 + (1-\alpha_2)B_1B_2} = \frac{sB_1}{D_1(s)}$	$\frac{V_{o2}}{V_{in}} = \frac{\alpha_1 B_1 B_2}{D_1(s)}$
17.33(b)	$\frac{V_{o1}}{V_{in}} = \frac{B_1(s+\alpha_2 B_2)}{s^2 + sB_2\alpha_2 + \alpha_1\alpha_2 B_1 B_2} = \frac{B_1(s+\alpha_2 B_2)}{D_2(s)}$	$\frac{V_{o2}}{V_{in}} = \frac{\alpha_1 B_1 B_2}{D_2(s)}$
	$\cong \frac{sB_1}{D_2(s)}$ if $\omega \gg \alpha_2 B_2$	

The circuits are basically suitable for low to medium Q values, for which it is required that by design:

$$C_1 > C_2 \text{ and } C_4 > C_3 \tag{17.98}$$

https://doi.org/10.1017/9781108762632.018 Published online by Cambridge University Press

Parameters can be tuned electronically, but passive tuning is interactive. An attractive feature is the low value of active and passive sensitivities of the filter parameters.

Medium to High *Q* Filters: Figure 17.34(a) and (b) are two representative OA-C circuits for the simultaneous realization of LP and BP responses. Analysis based on the approximated frequency dependent model of OAs gives the transfer function included in Table 17.4. Parameters of interest for these filters are given in Table 17.5.

Table 17.4 Voltage ratio transfer function of the filters of Figure 17.34(a) and (b)

Fig. No.	$H_{BP}(s) = V_{o1}/V_{in}$	$H_{LP}(s) = V_{o2}/V_{in}$
17.34(a)	$\dfrac{B_1\left(s + B_2C_3/C_{3-4}\right)}{s^2 + s(B_2C_3/C_{3-4}) + B_1B_2C_1/C_{1-2}} = \dfrac{B_1\left(s + B_2C_3/C_{3-4}\right)}{D_3(s)}$	$\dfrac{B_1B_2C_1/C_{1-2}}{D_3(s)}$
	$= \dfrac{sB_1}{D_3(s)}$ if $\omega \gg B_2C_3/C_{3-4}$	
17.34(b)	$\dfrac{sB_1C_1/C_{1-2}}{s^2 + s(B_1C_3/C_{3-4}) + B_1B_2C_2C_5/(C_{1-2}C_{5-6})} = \dfrac{sB_1C_1/C_{1-2}}{D_4(s)}$	$\dfrac{-B_1B_2C_2C_5/(C_{1-2}C_{5-6})}{D_4(s)}$

Table 17.5 Parameters of the filters of Figure 17.34(a) and (b)

Fig. No.	h_{LP}	h_{BP}	ω_o	Q
17.34(a)	1	$\dfrac{B_1}{B_2}\dfrac{C_{3-4}}{C_3}$	$\left(B_1B_2\dfrac{C_1}{C_{1-2}}\right)^{1/2}$	$\left(1+\dfrac{C_4}{C_3}\right)\left(B_1B_2\dfrac{C_1}{C_{1-2}}\right)^{1/2}$
17.34(b)	$-\dfrac{C_1}{C_2}$	$\dfrac{C_1}{C_{1-2}}\dfrac{C_{3-4}}{C_3}$	$\left(B_1B_2\dfrac{C_2}{C_{1-2}}\dfrac{C_5}{C_{5-6}}\right)^{1/2}$	$\left(1+\dfrac{C_4}{C_3}\right)\left(\dfrac{B_2}{B_1}\dfrac{C_2}{C_{1-2}}\dfrac{C_5}{C_{5-6}}\right)^{1/2}$

The filter of Figure 17.34(a) realizes the non-inverting LP response at the output of OA2 and gives mixed BP response at the output of OA1, which becomes near ideal BP response for $\omega >> B_2C_3/C_{3-4}$. Only four capacitors are used and the circuit parameters are in terms of capacitor ratios only. It has independent passive tunability of Q with C_3 and/or C_4. Circuits are suitable for medium Q filters; in the high Q case, component spread between C_3 and C_4 will become high.

The multifunctional filter of Figure 17.34(b) employs an additional pair of capacitors and provides ideal non-inverting BP and inverting LP characteristics at the output terminals of OA1 and OA2, respectively. Other aspects regarding tunability, component spread, etc., are similar to the previous circuit. Incremental sensitivities of both the filters are small.

https://doi.org/10.1017/9781108762632.018 Published online by Cambridge University Press

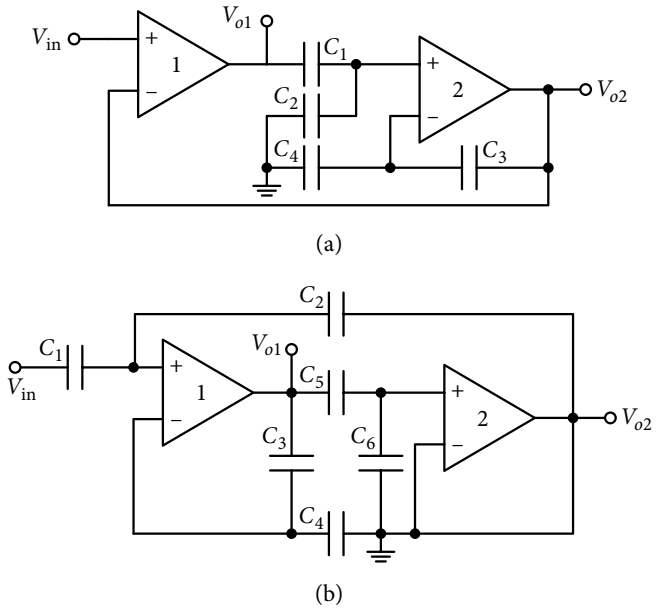

Figure 17.34 Medium to high-*Q* OA-C second-order low pass and band pass filter sections.

It is well-known in literature that a biquadratic building block can be realized from a second-order filter having two standard responses simultaneously. Techniques have been used in previous chapters and need not be repeated here. It can be successfully employed in the OA-C case, using circuits shown in Figures 17.33 and 17.34 or similar circuits.

Example 17.9: Design the second-order filter of Figure 17.34(b) which is to be used to realize BP and LP responses for a center frequency of 62.5 kHz having Q = 2, 5 and 10.

Solution: With B_1 and B_2 taken as $2\pi\ 10^6$ rad/s for 741 type OAs, to get center frequency of 62.5 kHz, the ratio of capacitors C_2/C_{1-2} and C_5/C_{5-6} each, are taken as 1/16 from Table 17.5. With these ratios of capacitors, ratio of C_4/C_3 becomes 31, 79 and 159 for Q = 2, 5, and 10, respectively. The selected value of the capacitors is as follows:

$$C_1 = 75 \text{ pF}, C_2 = 5 \text{ pF}, C_3 = 2 \text{ pF}, C_5 = 5 \text{ pF and } C_6 = 75 \text{ pF}$$

Values of C_4 = 62 pF, 158 pF, and 318 pF, respectively, are for increasing values of Q. For completing the path for dc biasing, high value resistances were connected across C_2, C_3 and C_5. It was observed that with these values of C_4, the value of Q was enhanced and trimming of either C_4 or C_3 was required. The values used for C_4 was 61 pF, 116 pF and 167 pF with the other capacitors remaining the same. Simulated responses of the BP and LP responses for the three values of Q, but with same value of center frequency, are shown in Figure 17.35(a) and (b). For the BP case in Figure 17.35(a), simulated center frequency and Q for the three cases are 64.3 kHz, 62.99 kHz and 62.99 kHz, and 2.16, 5.24, and 10.01, respectively. For

https://doi.org/10.1017/9781108762632.018 Published online by Cambridge University Press

the LP case of Figure 17.35(b), dc gain for the three cases is 15, and peak gain of 33.15, 77.65 and 149.3 occurs at 60.11 kHz, 62.33 kHz and 62.45 kHz; which corresponds to the cut-off frequency of 63.44 kHz, 62.92 kHz and 62.6 kHz, respectively.

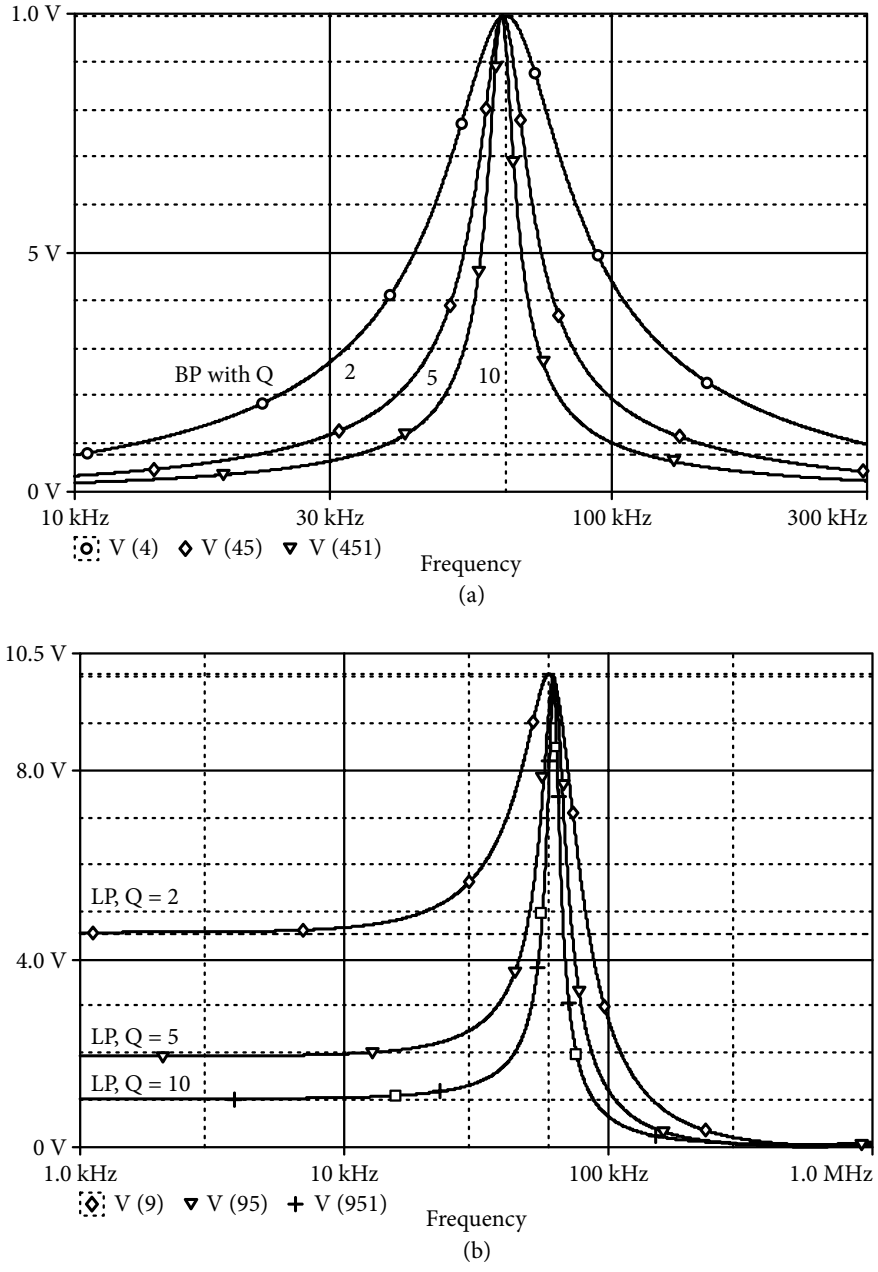

Figure 17.35 (a) Second-order band pass responses for the circuit in Figure 17.34(b) and (b) its low pass responses.

https://doi.org/10.1017/9781108762632.018 Published online by Cambridge University Press

17.16 Cascade Design

Cascade design has been discussed before in detail. In this section, a design example shall be taken to illustrate the technique for the OA-C case [17.16]. A fourth-order LP Butterworth filter is realized by cascading second-order LP sections of the circuit shown in Figure 17.34(a). The cascaded filter is shown in Figure 17.36(a), for which overall transfer function is given as:

$$H(s)=\frac{B_1B_2B_3B_4\left(\frac{C_1}{C_{1-2}}\frac{C_5}{C_{5-6}}\right)}{\left(s^2+sB_2\frac{C_3}{C_{3-4}}+B_1B_2\frac{C_1}{C_{1-2}}\right)\left(s^2+sB_2\frac{C_7}{C_{7-8}}+B_3B_4\frac{C_5}{C_{5-6}}\right)} \tag{17.99}$$

From equation (17.99), the pole frequency and pole-Q of the individual second-order section are, respectively, given as:

$$\omega_{o1}=\left(B_1B_2\frac{C_1}{C_{1-2}}\right)^{1/2},\ Q_1=\left(1+\frac{C_4}{C_3}\right)\left(\frac{B_1}{B_2}\frac{C_1}{C_{1-2}}\right)^{1/2} \tag{17.100}$$

$$\omega_{o2}=\left(B_3B_4\frac{C_5}{C_{5-6}}\right)^{1/2},\ Q_2=\left(1+\frac{C_8}{C_7}\right)\left(\frac{B_3}{B_4}\frac{C_5}{C_{5-6}}\right)^{1/2} \tag{17.101}$$

Then, the two sections are designed to realize fourth-order Butterworth response for cut-off frequency of 25 kHz. For the standard Butterworth denominator polynomial, the corresponding Q-values are available, which are: $Q_1 = 1.31$ and $Q_2 = 0.54$.

For 741 type OAs, $\omega_o/B = 1/40$, it gives, from equations (17.100) and (17.101):

$$(C_1/C_{1-2}) = (C_5/C_{5-6}) = (1/1600) \tag{17.102}$$

Application of relation in equation (17.102) in equation (17.100) and equation (17.101), gives:

$$(C_4/C_3) = 51.4 \text{ and } (C_8/C_7) = 20.6 \tag{17.103}$$

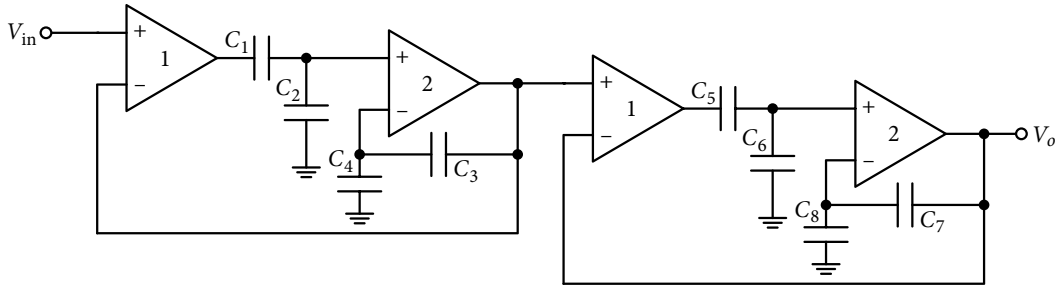

(a)

https://doi.org/10.1017/9781108762632.018 Published online by Cambridge University Press

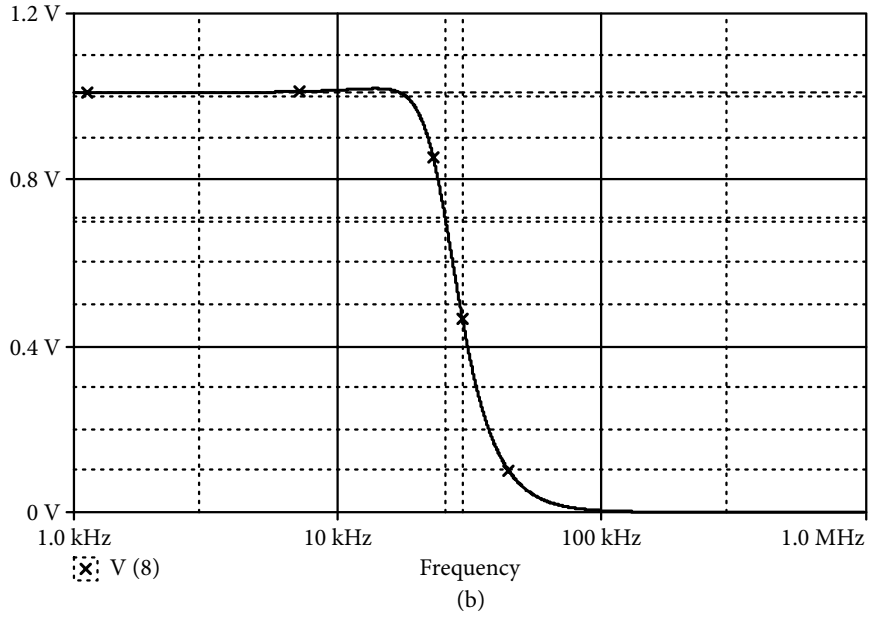

Figure 17.36 (a) Cascaded fourth-order OA-C low pass filter for equation (17.99) and (b) its simulated response.

The following values of capacitors were used for the relations in equations (17.102) and (17.103).

$$C_1 = 100 \text{ pF}, C_2 = 159.9 \text{ nF}, C_3 = 200 \text{ pF}, C_4 = 10.28 \text{ nF} \quad (17.104a)$$

$$C_5 = 100 \text{ pF}, C_6 = 159.9 \text{ nF}, C_7 = 200 \text{ pF}, C_8 = 4.12 \text{ nF} \quad (17.104b)$$

The realized filter with capacitor values was simulated, while 10 megΩ resistances were connected across C_1, C_4, C_5 and C_8. Simulated response is shown in Figure 17.36(b), having unity dc gain and cut-off frequency of 25.7 kHz.

Practical Considerations: There are many advantages in utilizing OA-R/ C circuits using the first-pole roll-off model of OAs. Circuit parameters are in terms of capacitor (or resistance) ratios and the frequency range of operation is appreciably extended. However, it is necessary to know and account for the various factors which affect the idealized behavior of the OA-R/ C filters.

In the practical fabrication of MOS-based filters, parasitic capacitors are always present. Their effect has to be reduced considerably through a proper layout of the system. In many designs, effort is made to assimilate parasitic capacitances with physically used capacitances.

It is necessary to provide complete dc path in active C circuits for input bias currents and dc stability. As has been shown in examples, a high value resistance is connected in parallel with the capacitors blocking the dc path.

https://doi.org/10.1017/9781108762632.018 Published online by Cambridge University Press

17.17 Effect of OA's Non-idealness on Active R and Active C Filters

Degradation in the performance of active RC networks using 741 type of OAs, especially beyond audio frequencies, is due to a number of reasons, including the limitations and non-idealness of OAs. The main reason for performance deviation at higher frequencies has now been shown to be significantly reduced in active R and active C circuits. As a result, the useful frequency range has been shown to be increased in examples. However, there are some other imperfections in OAs, which can affect filter performance. Obviously, the amount of non-idealness should be known, so that corrective measures may be taken.

Effect of Temperature and Bias Voltage Drifts: Dimensional considerations show the dependence of active R/C circuit parameters on the gain bandwidth of the OAs used in their realization. For example, in two OA second-order filters, the pole frequency ω_o, and quality factor Q are, respectively, proportional to $(B_1B_2)^{1/2}$ and (B_1/B_2). Similarly, in the simulation of inductance, FDNR and capacitance or resistance, the realized values and parameters are strongly dependent on bandwidths of the OAs. The bandwidth of a commercially available OA in ICs has large tolerance; it can be somewhere between 20% and 50%. In addition, it is sensitive to variations with respect to temperature and bias voltage drifts. In the temperature range $0°C \leq T \leq 70°C$, the variations in B may be as large as 20%; such changes in B are undesirable [17.17]. It is found that B is inversely proportional to temperature T but varies almost linearly with supply voltage. A combination of large tolerance and value drifts due to temperature and supply voltage variations in B makes active R and active C circuits unsuitable for practical applications unless corrective measures are taken.

Some of the important compensation/corrective methods for reducing the aforementioned problems are: (a) schemes using variations in capacitors or resistors to match the variations in B, (b) schemes using phase-lock ω_o stabilization and (c) schemes using temperature compensated OAs with regulated power supply. A combination of the two schemes can also be used for more stringent requirements.

Rao and Srinivasan [17.18] gave a simple yet effective method for the B-stabilization against temperature and bias voltage drifts. In another effective method for the stabilization of the bandwidth B, basically, the dependence of B on the bias conditions in an OA is used to overcome temperature drifts, either in (i) open-loop, or (ii) closed-loop. The closed-loop systems are superior and derive the actual monitored variation of $B(V, T)$, via ω_o by using phase-lock ω_o stabilization technique. The schemes are known as ω_o stabilization techniques and are given by a number of researchers [17.8].

The phase-lock loop ω_o stabilization techniques are a bit more complicated than the other schemes, and are clearly suited for systems of several filters, where they can be implemented in the inexpensive integrated form. They, however, provide excellent stabilization not only against temperature variations, but also against drifts in bias voltages and aging.

A simple and convenient method of B stabilization is the use of temperature compensated OAs. Such OAs, like LM 324 are commercially available and have about 3.5% variation in B over a range of 0-70° C. For bias voltage drifts, use of regulated supply is recommended.

https://doi.org/10.1017/9781108762632.018 Published online by Cambridge University Press

References

[17.1] Allen, P. E., and J. A. Means. 1972. 'Inductor Simulation Derived from an Amplifier Roll-Off Characteristic,' *IEEE Transactions* CT-19: 395–7.

[17.2] Siddiqi, M. A. 1979. 'Network Synthesis Using Internal Dynamics of Operational Amplifiers.' PhD. Thesis, Aligarh Muslim University, India.

[17.3] Siddiqi, M. A., and M. T. Ahmed. 1978. 'Active R Simulation of Lossy Inductor for High Frequency Applications,' *Proceedings of. IEEE IACAS (USA)* 924–6.

[17.4] Soliman, A. M. 1978. 'A Novel Inductor Simulation Using the Pole of the Operational Amplifier,' *Frequenz* 1 (32): 239–40.

[17.5] Siddiqi, M. A., and M. T. Ahmed. 1991. 'Direct Form Active R Synthesis and their Critical Assessment,' *International Journal of Electronics* 71: 621–35.

[17.6] Siddiqi, M. A., and M. T. Ahmed. 1979. 'Realization of Grounded Capacitor with Operational Amplifier and Resistance,' *Electronic Letters* 14: 633–4.

[17.7] Siddiqi, M. A., M. T. Ahmed., and I. A. Khan. 1980. 'Realization of a First-order Active R Network,' *23rd Midwest Symposium on Circuit and Systems*, Toledo.

[17.8] Brand, J., and R. Schaumann. 1978. 'Active R Filters: Review of Theory and Practice,' *IEE Journal of Electrical Circuits and Systems* 2: 89–101.

[17.9] Ahmed, M. T., and M. A. Siddiqi. 1978. 'Realization of Active R Biquadratic Circuit,' *12th Asilomar Conference of C.S. and Computers*, Montery (USA).

[17.10] Khan, I. A., and M. T. Ahmed. 1983. 'An Active C Resonator and its Applications in Realizing Monolithic Filters and Oscillators,' *Microelectronic Journal of England* 14 (1): 61–66.

[17.11] Ishida, M., T. Fukui, and Ebistuam. 1984. 'Novel Active R Synthesis of Driving Point Impedance,' *International Journal of Electronics* 56 (1): 151–8.

[17.12] Mitra, S. K. 1969. *Analysis and Synthesis of Linear Active Networks.* US: John Wiley.

[17.13] Schaumann, R., M. A. Soderstrand, and K. R. Laker. 1981. *Modern Active Filter Design*. New York: IEEE Press.

[17.14] Khan, I. A. 1987. 'Realization and Study of MOS-compatible Active C High Frequency Filters and Oscillators.' PhD Thesis, Aligarh Muslim University, India.

[17.15] Khan, I. A., and M. T. Ahmed. 1981. 'Realization of MOS Compatible First-order Active C Networks,' *Journal of IETE India* 27 (6): 204–6.

[17.16] Khan, I. A., and M. T. Ahmed. 1986. "Realization of a MOS Compatible Multifunctional Active C Biquadratic Filter for High Frequency Applications". *Microelectronic Journal of England* 17(4): 233–7.

[17.17] Fairchild Semiconductors. 1973. 'Linear Integrated Circuit Catalog.'

[17.18] Rao, K. R., and S. Srinivasan. 1974. 'A High Q Temperature Insensitive Band Pass Filter Using the Operational Amplifier Pole,' *Proceedings of IEEE* 2: 1713–4.

https://doi.org/10.1017/9781108762632.018 Published online by Cambridge University Press

Practice Problems

Note: OAs will be considered non-ideal, represented by its approximate model of equation (17.1), ($A \cong B/s$) with bandwidth $B = 2\pi \times 10^6$ rad/s.

17-1 (a) Figure P17-1 shows a passive BPF circuit. Design and test the filter circuit simulating the inductance employing GI-1 of Figure 17.1(a). Center frequency of the BPF is to be 5×10^5 rad/s and $Q_o = 5$.

(b) Explain the effect of any parasitic resistance in parallel with the simulated inductance L.

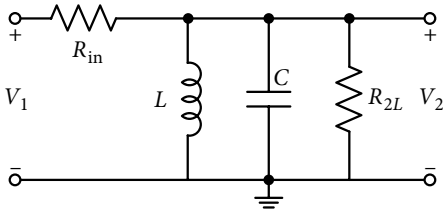

Figure P17-1

17-2 Show that the circuit shown in Figure P17-2 simulates a non-ideal GI. Obtain its equivalent circuit and the expression of the simulated GI and associated parasitic. Assume $R_1 = R_4$ and $(R_2/R_3) = k < 1$.

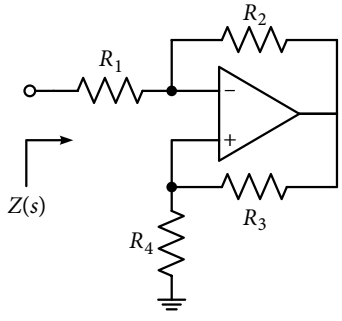

Figure P17-2

17-3 Employ the GI of Problem 17-2 to get a first-order HPF of Figure P17-3, having cut-off frequency of 4×10^5rad/s.

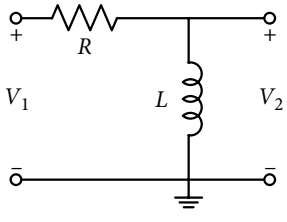

Figure P17-3

17-4 A 5 mH GI is to be simulated using the circuit of GI-1 shown in Figure 17.1(a). Plot its quality factor in the frequency range of $0.01 \le (\omega/B) \le 0.5$; assume $R_1 = 0$ and $(R_4/R_3) = (i)$ 1, (ii) 2 and (iii) 5. Explain the

https://doi.org/10.1017/9781108762632.018 Published online by Cambridge University Press

effect of these values of the resistance ratio (R_4/R_3) on the variation of the quality factor of the simulated inductance.

17-5 Low component FI-2 of Figure 17.4(a) is modified as shown in Figure P17-4. Show that it still realizes inductance L_p in parallel with a parasitic resistance R_p with the following expressions for these parameters:

$$L_p = \frac{kR}{B}, R_p = \frac{k}{1+k}R \text{ and } Q = \frac{B}{\omega(1+k)}$$

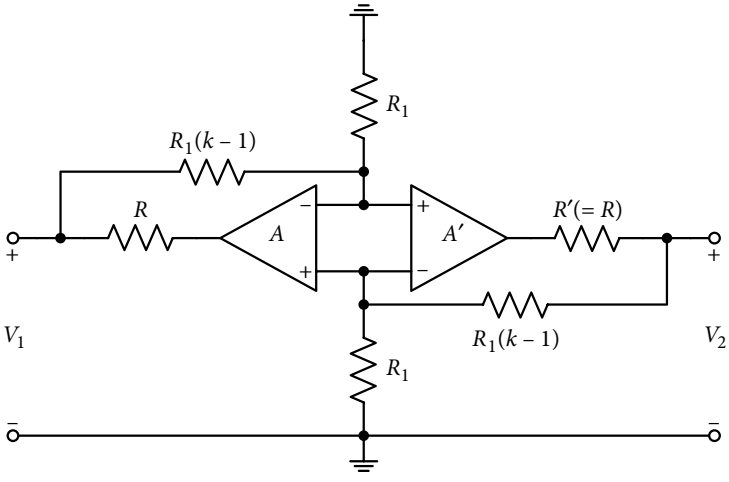

Figure P17-4

17-6 Design and test a sixth-order LP Butterworth filter using FI-2 of Figure 17.4(a) having pass band edge frequency of 100 krad/s and 0 dB gain at dc.

17-7 Design and test a sixth-order LP Chebyshev filter using FI-2 of Figure 17.4(a) having a pass band edge frequency of 120 krad/s and ripple width of 0.1 dB. What is the attenuation at 150 krad/s?

17-8 Redesign the sixth-order LPF for Problem 17-7 using the grounded FDNR of Figure 17.7(a).

17-9 Show that the circuit in Figure P17-5 realizes a second-order notch filter. Design the filter using floating capacitor of Figure 17.12 and floating inductor of Figure 17.4. Frequency of the notch is to be 100 kHz. Assume a suitable value for the load resistance and find the attenuation at the notch frequency.

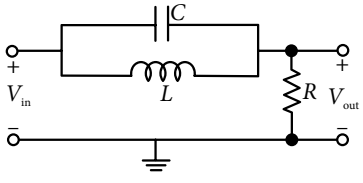

Figure P17-5

https://doi.org/10.1017/9781108762632.018 Published online by Cambridge University Press

17-10 Figure P17-6 shows a second-order passive prototype LPF. Design it having Butterworth characteristics with a cut-off frequency of 10^5 rad/s. Replace the inductor and capacitor to obtain a fully active R version of the circuit and verify it using PSpice. The high-quality GC simulator of Figure 17.11 may be used.

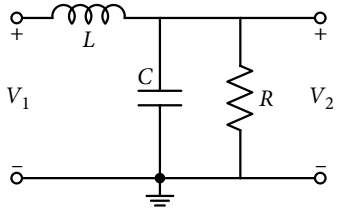

Figure P17-6

Note: Problems 17-11 to 17-13 are based on the realization of second-order filters using the basic scheme shown in Figure 17.15.

17-11 If the output is taken at terminal 2, show that the realized filter is a mixed HP, for which transfer function is given here, provided the following selection is used: elements $G_1 = G_3 = G$, $G_2 = G_4 = (k_1 G_1)$ and the parameters in equations (17.55–17.58) as $b_1 = b_3 = 0$, and $b_2 = (1 - a_3)$.

$$H_{HP}(s) = k_2 \frac{s^2 + k_1(1-a_1)Bs}{s^2 + k_1 k_2 a_2 Bs + \left(k_1^2 a_3^2 B^2/1 + 3k_1 + k_1^2\right)}$$

where, $k_2 = \dfrac{1+k_1}{1+3k_1+k_1^2}$

17-12 If the output is taken at terminal 2, show that the realized filter is a BEF with $H_{BE}(s)$ given here, provided the following selection is used: elements $G_1 = G_2 = G_3 = G_4 = G$ and the parameters in equations (17.55–17.58) as $a_2 = 0$, $b_1 = 2(1 - a_1) + b_3$ and $b_3 = (1/3)(1 - b_2)$.

$$H_{BE}(s) = \frac{2}{5} \frac{\left[s^2 + (1-a_1)a_3 B^2 + \left\{(1-b_2)(1+a_3-a_1)/6\right\}\right]}{s^2 + \dfrac{a_3 B^2}{5} s + \dfrac{a_3(1-b_2)B^2}{5}}$$

17.13 Using OA with $B = 2\pi \times 10^6$ rad/s, design a BR filter with notch frequency of 50 kHz and $Q = 5$, when the output is taken at terminal 3 in Figure 17.15.

17-14 Derive the driving point function for the circuit in Figure P17-7 and find the expression for the elements in the obtained equivalent circuit. Utilize it in the formation of a second-order BP filter with center frequency of 50 kHz and $Q = 2.5$.

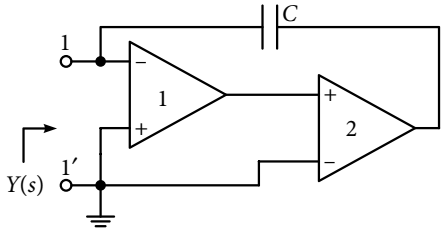

Figure P17-7

https://doi.org/10.1017/9781108762632.018 Published online by Cambridge University Press

17-15 Show that the circuit in Figure P17-8 simulates a parallel combination of a resistance, inductance and a capacitance.

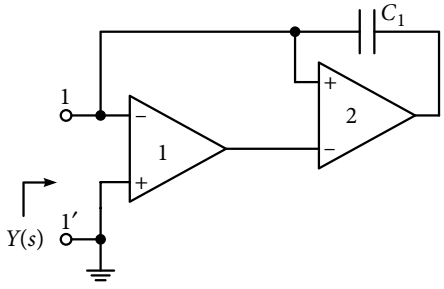

Figure P17-8

17-16 Derive the driving point function for the circuit in Figure P17-9. Use it to design a second-order BP filter for a center frequency of 50 kHz and $Q = 5$. Connect a capacitor attenuator between terminals A and B such that center frequency of the filter enhances to 100 kHz.

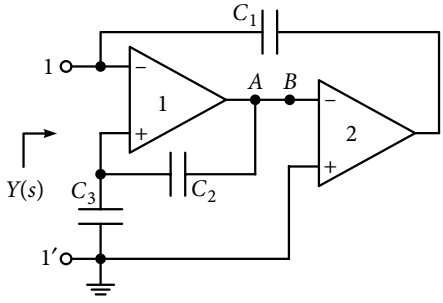

Figure P17-9

17-17 Show that the circuit of Figure P17-10 simulates a grounded FDNR. Find the expression for the FDNR and parasitic elements.

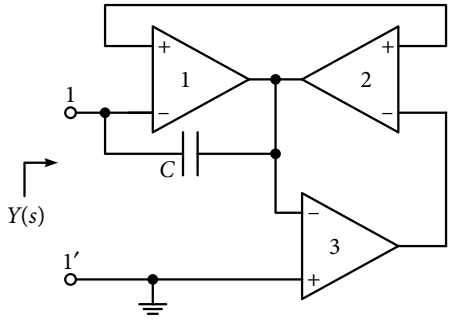

Figure P17-10

https://doi.org/10.1017/9781108762632.018 Published online by Cambridge University Press

17-18 Show that the circuit of Figure P 17-11 simulates a grounded FDNR. Find the expression for the FDNR and parasitic elements.

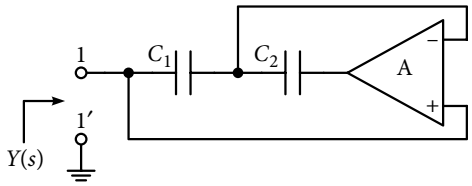

Figure P17-11

17-19 Derive the input admittance function for the circuit in Figure P17-12 when $B_1 = B_2$.

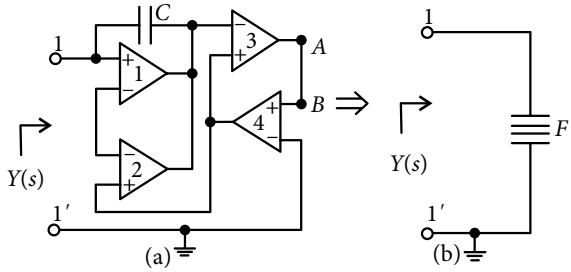

Figure P17-12

17-20 Design and test a second-order BE filter using the circuit shown in Figure 17.26(c) for having notch frequency of 62.5 kHz and $Q = 4$. Also find the maximum value of voltage gain and the frequency at which it occurs for a simultaneously obtained BP response from the circuit.

17-21 Design and test a second-order OA-C APF using the circuit shown in Figure P17.13 having phase shift of 90° at a frequency of 100 kHz.

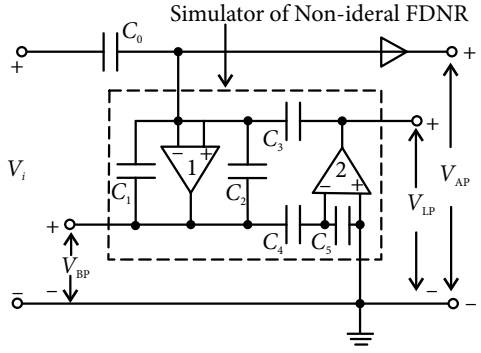

Figure P17-13

https://doi.org/10.1017/9781108762632.018 Published online by Cambridge University Press

17-22 Design and test a second-order Butterworth OA-C HPF using the circuit shown in Figure 17.28(b) having a cut-off frequency of 50 kHz.

17-23 Design and test a second-order LPF using the circuit shown in Figure 17.30(c) having 3 dB frequency of 125 kHz and $Q = 2.5$.

17-24 Design and test a first-order OA-C AP section of Figure 17.32(b), such that its phase becomes $-270°$ at $2\pi \times 100$ krad/s.

17-25 Design and test a third-order Butterworth OA-C filter using cascade approach having cut-off frequency of 100 krad/s.

https://doi.org/10.1017/9781108762632.018 Published online by Cambridge University Press